PHYSICSAccess Research Paper
ISSN Online: 2756-3898, ISSN Print: 2714-500X https://doi.org/10.47514/phyaccess.2023.3.2.013

Integration of Geologic and Geoelectrically Derived Parameters for Aquifer Vulnerability Assessment in Akure Metropolis, Southwestern Nigeria

Adeyemo I Adedotun[1], Boluwade B Stella[1], Sanusi S Olumide[1] and Akande V Oluwatimilehin[1]

[1] Department of Applied Geophysics, Federal University of Technology, Akure, Nigeria

Corresponding E-mail: iaadeyemo@futa.edu.ng

Received 16-11-2023
Accepted for publication 13-12-2023
Published 14-12-2023

Abstract

Assessment of aquifer vulnerability was carried out in the northwestern part of Akure, Southwestern Nigeria where the presence of automobile workshops is the major source of pollution using integrated methods of multi-criteria approach and physico-chemical investigations. 187 vertical electrical sounding (VES) data were acquired using the Schlumberger array technique with (AB/2) ranging from 65 - 150 m. Six geologic and geoelectric parameters; surface elevation, lithology, aquifer overlying layer resistivity, aquifer overlying layer thickness, coefficient of anisotropy and hydraulic conductivity were combined to develop an aquifer vulnerability model (AVM) for the study area using the GIS technique. These factors were subjected to the Fuzzy Analytical Hierarchy Process (FAHP) method of weightage determination to assign weights to each criterion of the aquifer vulnerability conditioning factors (AVCFS) using GIS. The AVM shows that the eastern and western flanks of the study area are of moderate to high vulnerability, while the central area is mainly of very low to moderate vulnerability. Fifteen (15) water samples were obtained from wells across the area for physico-chemical analyses. The predicting accuracy of the aquifer vulnerability model was validated using one of the physiochemical parameters determined from water samples collected across the area (lead) and longitudinal conductance. The validations from the two approaches produced an accuracy of 73% and 74% respectively which proved the reliability of the model. The produced aquifer vulnerability map can be used for precise decision-making processes in environmental planning and groundwater management in the study area.

Keywords: Aquifer vulnerability model; Fuzzy Analytical Hierarchy Process; Longitudinal Conductance; Physicochemical; Lead.

I. INTRODUCTION

Groundwater quality has been under threat directly and indirectly by human activities [1]. Groundwater is susceptible to contamination and pollution from both natural and anthropogenic sources [1, 2]. Geometric growth and geographic spread of the human population have resulted in groundwater contamination through irregular planning, urban sprawl, the use of chemical products, and improper sewage disposal systems including sewage from industry, agriculture, and urban areas which are directly washed into groundwater systems [3, 4, 5, 6, 7, 8, 9]. Notable among industrial waste

often released to the ground are hydrocarbon-oil, such as diesel oil, petrol and used lubricant oil [10]. Consumption of contaminated water could result in a variety of waterborne diseases (such as Diarrhea, Cholera, Dysentery and Typhoid), gastrointestinal illness, reproductive problems and neurological disorders [11], especially in children and pregnant women.

Aquifer vulnerability assessment is important to predict areas of potential risk of contamination [12]. The susceptibility of groundwater to contamination and the function of pollutant properties, anthropogenic activities, and physical parameters is termed 'Aquifer Vulnerability' [13]. Vulnerability information can aid in the choice of proper locations for certain activities so that the adverse effects on groundwater are minimized and thus protect the groundwater resources [14]. Aquifer vulnerability assessment is therefore crucial for groundwater resources management and land-use planning [13, 15]. This approach has largely enhanced groundwater resource sustainability in the field of groundwater hydrology [16, 17]. The study area is within the basement complex of southwestern Nigeria where the aquifer layer usually exists within shallow subsurface thus making the infiltration of leachate possible [18, 19, 20].

The major source of pollution in the area is the automobile mechanic workshops which concentrate in the northeastern and eastern parts. The age of each of the automobile workshops was established through interactions with their operators to be about 25 - 35 years old. The biodegradation of these wastes generates leachate plumes that can contain both chemical and biological constituents [21, 22]. These leachates are typical sources of groundwater contamination especially where they infiltrate the subsurface layers to pollute the aquifer system. The increasing growth rate of houses, human activities and the continuous discharge of hydrocarbon-based waste in some parts of the study area could pose a threat to the groundwater resources in the area, especially since the groundwater flow was not taken into consideration before siting these auto-mechanic workshops [23].

Groundwater vulnerability assessments have been well evaluated by constructing aquifer/groundwater vulnerability maps [24, 25]. The Electrical Resistivity (ER) method is widely used in solving groundwater contamination problems [26, 27]. Some of the advantages of ER are its high data resolution and cost-effectiveness. It is equally useful in mapping continuous subsurface information along a profile [28, 29]. Geoelectrically derived parameters can be used in describing the hydrological condition of the subsurface and its aquifer protective capacity rating [30]. Subsurface contamination due to oil spills and oil-based leachate can be detected, mapped and modelled using resistivity methods because oil-contaminated land often possesses electrical resistivity anomalies that are different from equivalent but uncontaminated land [31].

Several environmental studies involving the use of Multi Criteria Decision Analysis (MCDA) have been carried out [32, 33, 34, 35, 36, 37, 38, 39, 40, 41, 42, 43]. One of the most widely used MCDAs is the Analytical Hierarchy Process (AHP). The AHP is a subjective method for analyzing qualitative criteria to weigh the alternatives. The AHP depends on expert knowledge/judgments, and it is always accompanied by uncertainty [44, 45]. This contributes to the imprecise judgments of decision-makers in the pair-wise comparison process [46].

To overcome this uncertainty and make a more precise decision, the Fuzzy Analytical Hierarchy Process (FAHP) was proposed for solving the hierarchical problems [47]. The fuzzy AHP technique can be considered as an advanced analytical method developed from the traditional AHP. The fuzzy AHP method determines the weight of the criteria in which the expert's subjective judgments are established through a two-to-two comparison. In this method, comparisons are expressed using triangular numbers whose expansion indicates the uncertainty of a given judgment [32]. Decision makers find it more reliable to give interval judgments than fixed values [45, 48]. The major advantage of Fuzzy AHP methods is that they can be used for both qualitative and quantitative criteria and they enable decision-makers to deal with inconsistent judgments systematically [49]. FAHP gives more credibility and confidence to the judgments of experts [32]. The multi-criteria decision analysis (MCDA) technique is greatly enhanced by employing the GIS technique, which is an important tool for the effective management of several vulnerability parameters [38, 50].

The research aims to evaluate the vulnerability of aquifer layers in the study area to possible contamination arising from human activities in the study area. To achieve this aim, the study delineated the subsurface geo-electric sequence underlying the study area and determined the aquifer vulnerability conditioning factors such as surface elevation, lithology, overlying layer resistivity, overlying layer thickness, coefficient of anisotropy and hydraulic conductivity. These parameters were integrated to produce an aquifer vulnerability model (AVM) map. The AVM was validated using longitudinal conductance and physiochemical analysis results to evaluate the efficiency of the model.

The survey area is in the northwestern part of Akure metropolis, Southwestern Nigeria. The area lies between longitude 737250 - 739250 mE and latitude 804300 - 807300 mN of the Universal Traverse Mercator system (UTM) Zone 31 (Fig. 1). The study area is moderately undulating with surface elevations ranging from 334 - 386 m above mean sea level (Fig. 1). The area is characterized by wet (April to October) and dry (November to March) seasons and mean annual rainfall ranges between 1500 and 2100 mm. The annual temperature ranges from 21 - 29^0C [51] and humidity is relatively high. The vegetation is of tropical rain forest which is characterized by thin forest. Access to the study area is through the interconnectivity of roads and footpaths. The geology of the area is characterized by rocks of the Basement Complex of Southwestern Nigeria [52]. The major rock types

found in the study area include charnockite, porphyritic granite, granite and quartzite (Fig. 2).

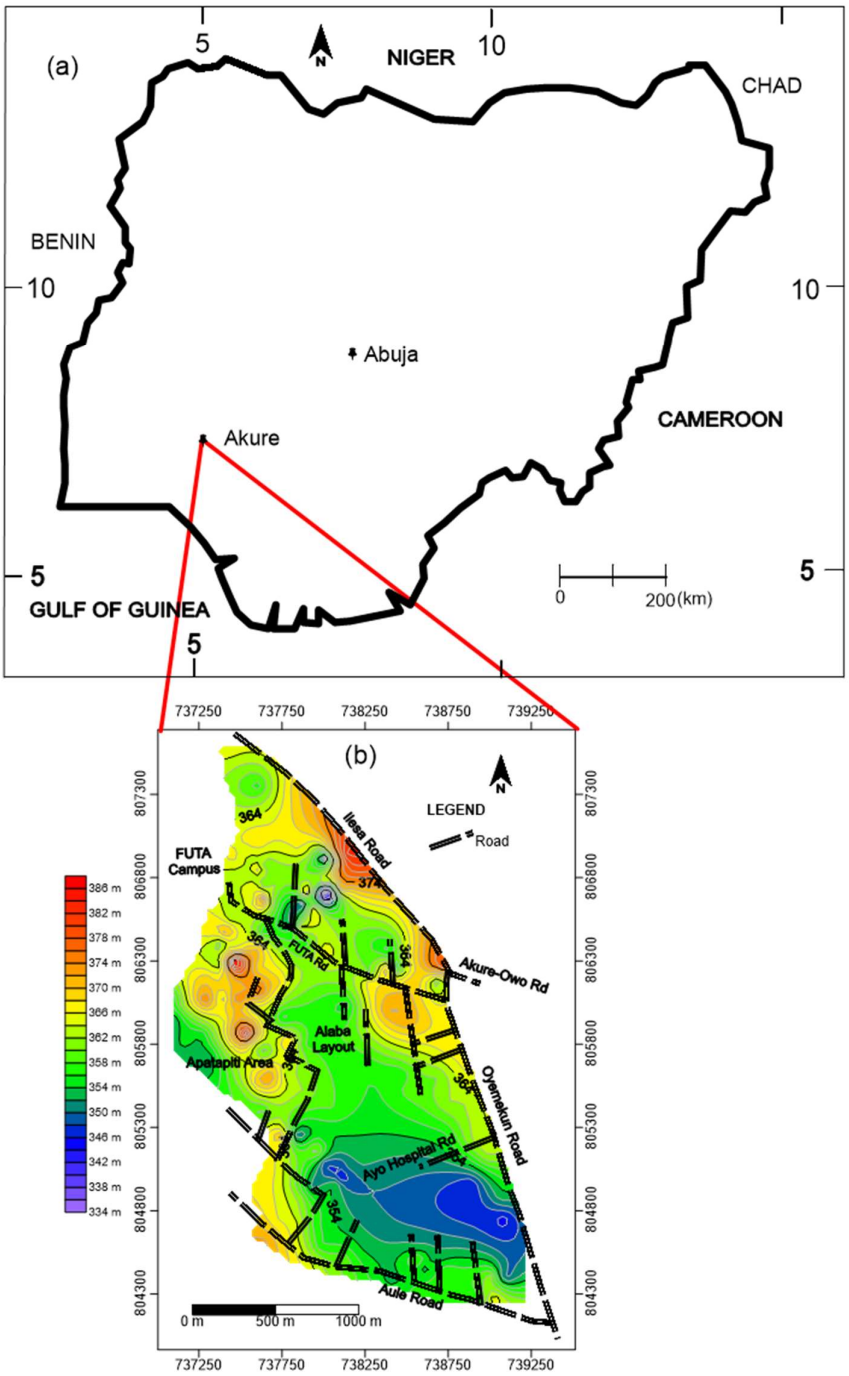

Fig. 1(a) Sketch map of Nigeria, (b) Base map of the study area showing elevation.

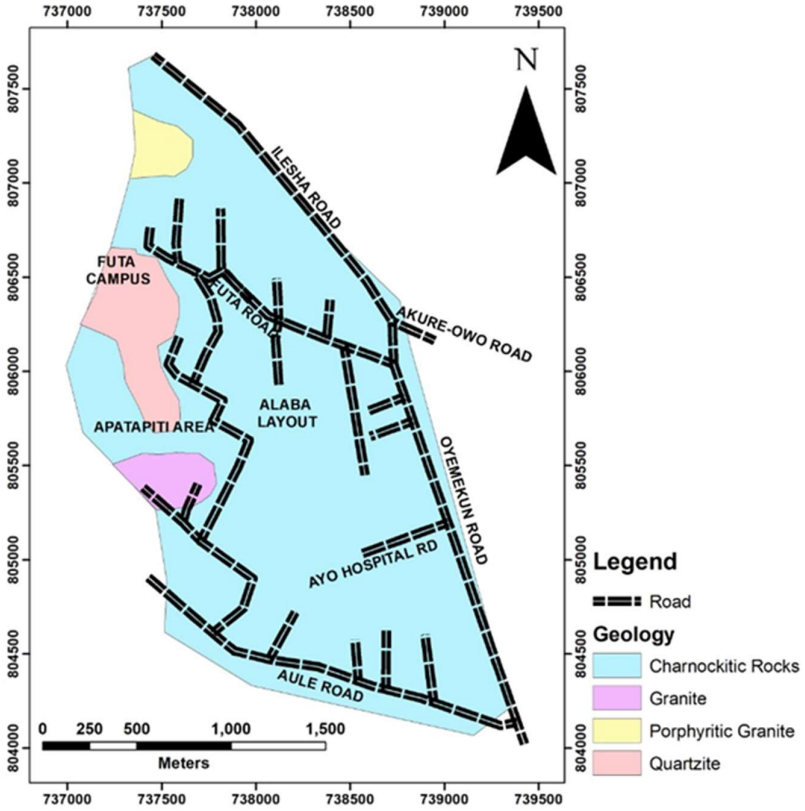

Fig. 2 Geological map of the study area.

II. METHODS

This study combines three data sources (Fig. 3); geoelectric, elevation and lithologic. 187 VES data were acquired (Fig. 4) using the Schlumberger electrode array [53]. The VES data were interpreted with a partial curve matching method [54] and WINRESIST version 1.0 [55] was used for the forward modelling of the initial geoelectric parameters (layer resistivity (ρ) and layer thickness (h). Geological mapping of the area was carried out to produce a reliable geological map of the area since the existing one is of low scale. Fifteen (15) water samples (Fig. 5) were collected from hang-dug wells across the area and the samples were analyzed to determine their physico-chemical parameters. Six parameters consisting of surface elevation, lithology, aquifer overlying layer resistivity, aquifer overlying layer thickness, coefficient of anisotropy and hydraulic conductivity were integrated to develop an AVM map for the study area. The AVM map was later compared with longitudinal conductance and lead concentration maps of the area to determine the efficacy of the AVM.

A. Aquifer Vulnerability Conditioning Factors (AVCFs):

The significance of these AVCFs parameters towards vulnerability is explained as follows: Elevation affects surface run-off. Elevation (Elev) helps to control the likelihood that a pollutant will run off or remain on the surface in one area long enough to infiltrate the underlain aquifer unit [56]. Water is more likely to infiltrate in low slope areas. Surface runoff is less in these areas allowing a high possibility of pollutant infiltration while areas with steep slopes enhance large amounts of runoff with low residence time for infiltration [57]. High infiltration increases the vulnerability of groundwater while low infiltration reduces the vulnerability of groundwater.

Lithology is an important hydrogeologic parameter that determines the amount of protection that the overlying layer(s) can offer the underlying aquifer layer. Thus, the lithology of an area can influence the vulnerability of the groundwater in such an area to a greater extent. Four different rock types were mapped in the study area, quartzite, porphyritic granite, granite and charnockite. The age, and degree of weathering and fracturing/faulting of these rocks affect the ease with which pollution can percolate through them.

The overlying layer thickness (OLT) refers to the vertical distance the pollutant will cover before getting to the groundwater. The thicker the OLT the lower the vulnerability of the aquifer layer [39, 43].

Hydraulic conductivity (K) is one of the most variable and yet the most important parameters in the estimation of contaminant travel time. This refers to the ability of the aquifer materials or overlying layer to transmit water; hence, it

controls the passage and attenuation of the contaminant material to the saturated zone [58, 59]. The movement of fluid within the aquifer rock materials is largely controlled by hydraulic conductivity. This factor controls the contamination degree within an aquifer medium at the rate of groundwater flow. Aquifers with high hydraulic conductivity values are most at risk of contamination [57, 60].

The hydraulic conductivity was estimated using (1) [61].

$$K = 0.0538e^{-0.0072} \quad (1)$$

Where ρ the apparent resistivity and K is the hydraulic conductivity.

The coefficient of Anisotropy is a measure of the degree of the earth's inhomogeneity which may result from fracturing, discontinuities or the presence of clay [62]. In a typical basement terrain, this electrical effect is due to near-surface features such as variable degrees of weathering and structural features like faults, fractures, joints, foliations and beddings. High values of the coefficient of anisotropy suggest that the fracture system must have extended in all directions with different degrees of fracturing while low values suggest uni-directional fracture [63]. If the total thickness of the layers in the geoelectric section considered is H, then the average longitudinal resistivity ρ_L is given by (2).

$$\rho_L = \sum_{i=1} \frac{h_i}{s_i} \quad (2)$$

Where h_i is the layer thickness and s_i is total longitudinal conductance.

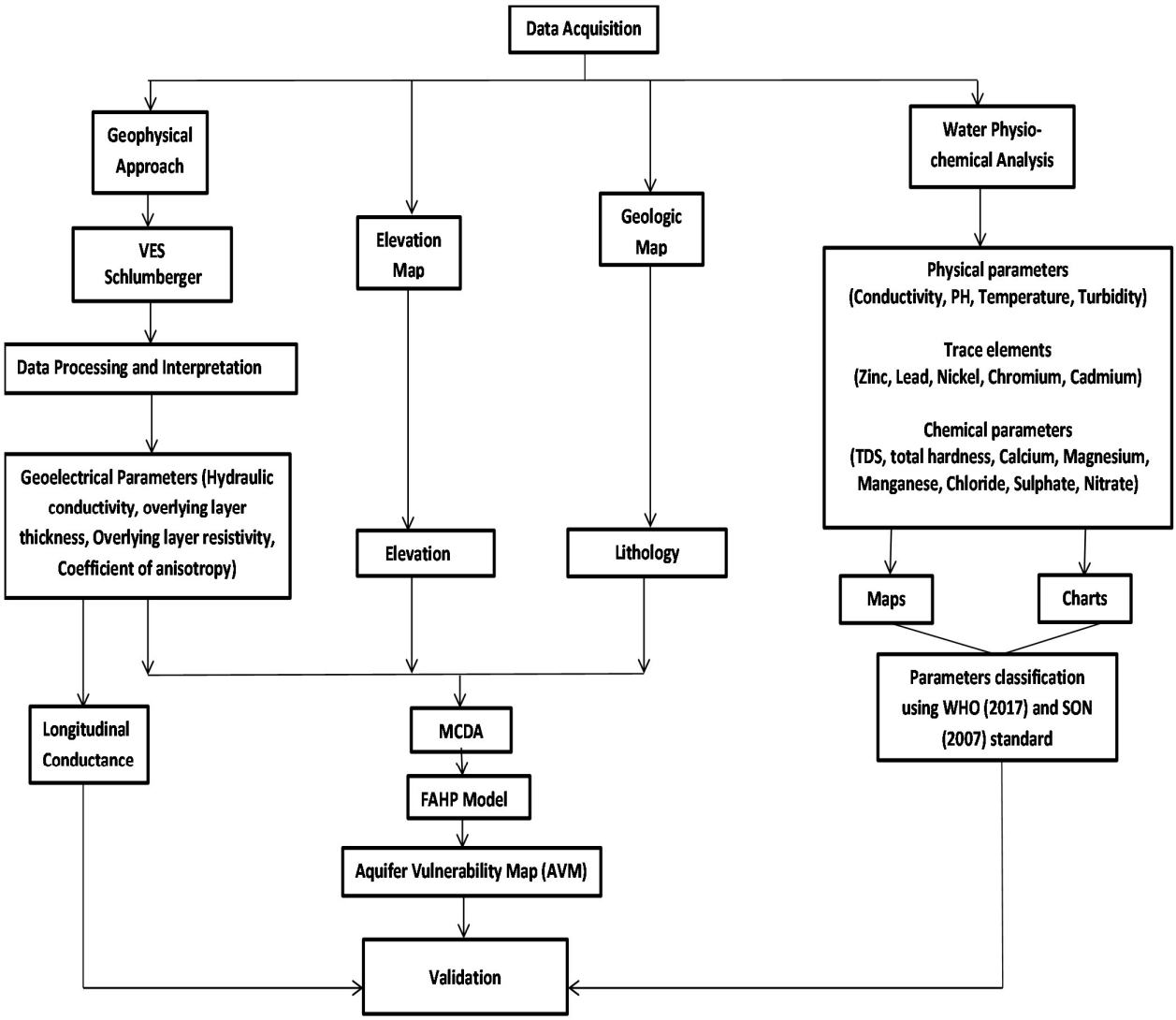

Fig. 3 Methodology Flow Chart for Aquifer Vulnerability Evaluation

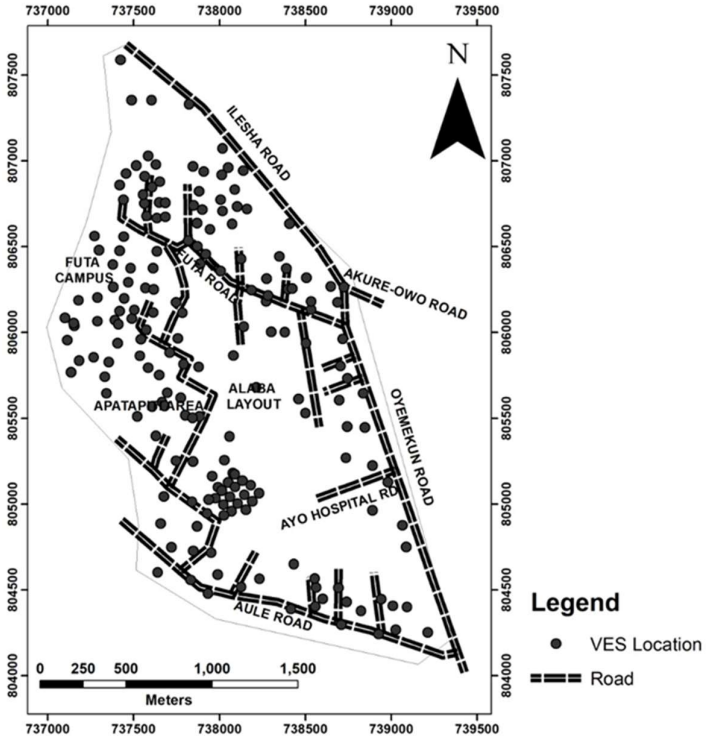

Fig. 4 Map of the Study Area Showing VES Station.

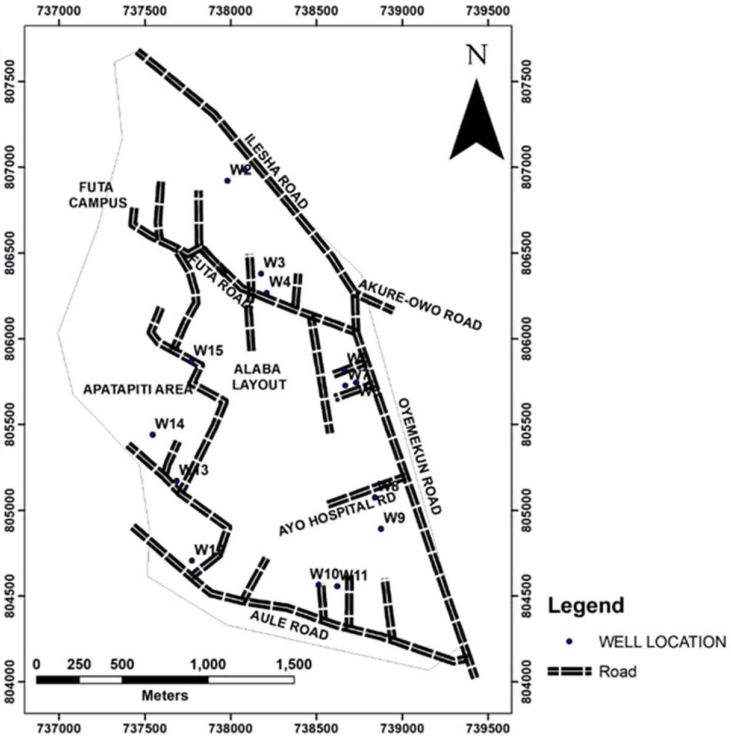

Fig. 5 Map of the Study Area Showing Water Sampling Locations

The average transverse resistance ρ_T is given by (3).

$$\rho_T = \sum \frac{T_i}{h_i} \quad (3)$$

Where, hi is the layer thickness and T_i is the total transverse resistance ρ_T is always greater than ρ_L. Therefore, the entire section will be anisotropic with regard to electrical resistivity. The coefficient of electrical anisotropy is defined as in (4).

$$\lambda = \left(\frac{\rho_t}{\rho_l}\right)^{1/2} \quad (4)$$

Where λ is real and greater than 1, ρ_t is transverse resistance and ρ_l is longitudinal conductance.

B. Fuzzy Analytic Hierarchy Process (FAHP)

APH method is one of the MCDAs introduced by Saaty in 1980 based on the subdivision of the problem in a hierarchical form. This technique is suitable for dealing with complex systems related to choosing among several alternatives with different objectives and criteria. AHP is a subjective method widely used in MCDA to determine appropriate weights for various criteria which are independent of the depth of the hierarchy [32]. At each level of the hierarchy, the AHP uses pairwise comparisons to estimate the relative priorities of criteria and alternatives. AHP has been effectively combined with other tools such as multi-objective mathematical programming aside from its use as a stand-alone decision tool [64]. Although, the AHP captures the expert's knowledge but lacks the benefits of handling vagueness in judgements during the conversion of verbal scales into a numeric scale [65].

To overcome all these drawbacks, a fuzzy upgrade of AHP called the Fuzzy-Analytic Hierarchy Process **(**FAHP**)** was developed to solve the fuzzy hierarchical problems more effectively for the uncertainty, inaccuracy, and ambiguity in expert judgments [66, 67, 68]. FAHP method has been used in determining the weights of the criteria by decision makers and then ranking of the methods has been determined by conventional AHP method. In the process of calculating FAHP, Chang's extent analysis method was adopted [69] to calculate the weights. The FAHP method determines the weight of the criteria primarily according to the subjective judgments of experts through a two-to-two comparison. In this method, pairwise comparisons are made using triangular numbers whose expansion indicates the uncertainty of a particular judgment [32]. The scale for pairwise comparisons of one attribute over another in the FAHP method can be seen in Table I [70]. The numbers were used as fuzzy scaling ratios, corresponding to the strength of preference for one element over another with interval values.

The application steps of the FAHP method were divided into 5 steps [71]. The steps for calculating the relative weight of each criterion in the FAHP method proposed by Chang's extent analysis [69] are as follows:

Let X = $\{x_1, x_2 \dots \dots, x_n\}$ be an object set and G = $\{g_1, g_2, \dots, g_n\}$ be a goal set. Using the method of Chang's extent analysis, each object is taken and the extent analysis for each goal is performed respectively. Therefore, extent analysis (m) values for each object can be obtained with the following notations:

$M_{g_i}^1, M_{g_i}^2, \dots, M_{g_i}^m, i = 1, 2, \dots, n$

Where $M_{g_i}^j (j = 1, 2, \dots, m)$ are triangular fuzzy numbers (TFNs).

Step 1: Let $(M_{g_i}^1, M_{g_i}^2, \dots, M_{g_i}^m)$ be values of extent analysis of the i[th] object for m goals. The value of fuzzy synthetic extent with respect to the ith object is defined using the algebraic operations on triangular fuzzy numbers as follows:

$$S_i = \sum_{j=1}^m M_{g_i}^j \left[\sum_{i=1}^n \sum_{j=1}^m M_{g_i}^j\right]^{-1} \quad (5)$$

To obtain $\sum_{j=1}^m M_{g_i}^j$, the fuzzy addition operation of m extent analysis values for a particular matrix is performed as follows:

$$\sum_{j=1}^m M_{g_i}^j = \left(\sum_{j=1}^m l_j, \sum_{j=1}^m m_j, \sum_{j=1}^m u_j\right) \quad (6)$$

To obtain $\left[\sum_{j=1}^n \sum_{j=1}^m M_{g_i}^j\right]^{-1}$ the fuzzy addition operation of $M_{g_i}^j (j = 1, 2, \cdots, m)$ values is performed such as,

$$\sum_{i=1}^n \sum_{j=1}^m M_{g_i}^j = \left(\sum_{i=1}^n l_i, \sum_{i=1}^n m_i, \sum_{i=1}^n u_i\right) \quad (7)$$

The inverse of the vector above is calculated, such as

$$\left[\sum_{i=1}^n \sum_{j=1}^m M_{g_i}^j\right]^{-1} = \left(\frac{1}{\sum_{i=1}^n u_i}, \frac{1}{\sum_{i=1}^n m_i}, \frac{1}{\sum_{i=1}^n l_i}\right) \quad (8)$$

Table I. Fuzzy scales of relative importance [70]

Scale for Importance	Triangular Fuzzy Scale	Triangular Fuzzy Reciprocal Scale
Just Equal	(1, 1, 1)	(1, 1, 1)
Equal Important (EI)	(1/2, 1, 3/2)	(2/3, 1, 2)
Weakly more Important (WMI)	(1, 3/2, 2)	(1/2, 2/3, 1)
Strongly more Important (SMI)	(3/2, 2, 5/2)	(1/3, 2/5, ½)
Very Strongly More Important (VSMI)	(2, 5/2, 3)	(1/3, 2/5, ½)
Absolutely More Important (AMI)	(5/2, 3, 7/2)	(2/7, 1/3, 2/5)

Step 2: For two triangular fuzzy numbers $M_1 = (l_1, m_1, u_1)$ and $M_2 = (l_2, m_2, u_2)$, the degree of possibility of $M_2 \geq M_1$ is defined as follows:

$$V(M_2 \geq M_1) = \underbrace{sup}_{y \geq x} \left[\min\left(\mu_{m_1}(x), \mu_{m_2}(y)\right)\right] \quad (9)$$

$$\tilde{A}^{-1} = (\mathrm{l, m, u})^{-1} = \left(\frac{1}{u}, \frac{1}{m}, \frac{1}{l}\right) \quad (10)$$

Where sup represents supremum, x & y are the values on the axis of membership function of each criterion. V $(M_2 \geq M_1)$ = 1. Since M_1 and M_2 are convex fuzzy numbers defined by the TFNs (l_1, m_1, u_1) and (l_2, m_2, u_2) respectively, it follows:

$$V(M_2 \geq M_1) = \mathrm{hgt}\,(M_1 \cap M_2) = \mu_{m_2}(x_d) \quad (11)$$

This expression can be equivalently written as follows:

$$V(M_2 \geq M_1) = \mathrm{hgt}\,(M_1 \cap M_2) = \mu_{M2}(\mathrm{d})$$
$$\begin{cases} 1, & if\ M_2 \geq M_1 \\ 0, & if\ l_1 \geq u_2 \\ \frac{l_1 - u_2}{(m_2 - u_2) - (m_1 - l_1)}, & otherwise \end{cases} \quad (12)$$

Where hgt is the height of fuzzy numbers on the intersection of M_1 and M_2, and d is the ordinate of the highest intersection point between μ_{M_1} *and* μ_{M_2} to compare M_1 and M_2, we need both the values of $V(M_1 \geq M_2)$ and $V(M_2 \geq M_1)$.

For $M_1 = (l_1, m_1, u_1)$ and $M_2 = (l_2, m_2, u_2)$, (5) is the possible ordinate of their intersection, from (6), we can obtain the degree of possibility for a convex fuzzy number.

Step 3: The degree possibility for a convex fuzzy number M to be greater than K convex fuzzy Mi (i = 1, 2, ..., k) numbers is given using the operations max and min [72] and is defined as:

$$V(M \geq M_1, M_2, \ldots, M_k) = V[(M \geq M_1)\ and\ (M \geq M_2)\ and \ldots and\ (M \geq M_k)] = \min V(M \geq M_I), i = 1, 2, \ldots, k \quad (13)$$

Step 4: In this step, the non-normalized weight vector was obtained by calculating the minimum value of V calculated in the previous step.

Assume that $d'(A_i) = \min V(S_i \geq S_k)$, where $k = 1, 2, \ldots, n$, $k \neq i$, and n is the number of criteria as described previously. Then, a weight vector is given by (14):

$$W' = (d'(A_1), d'(A_2), \ldots, d'(A_m)) \quad (14)$$

Where A_i (i=1,2, …, m) are m elements, each $d'(A_i)$ value represents the relative preference of each decision alternative. Then via the normalization process, vector W' is obtained, normalized and denoted as:

$$W' = (d'(A_1), d'(A_2), \ldots, d'(A_m)^T \quad (15)$$

Where A_i = (i= 1; 2; . . .. . .; n) are n elements.

Step 5: The Final stage; with normalization, the normalized weight vector is given as,

$$W = (d(A_1), d(A_2), \ldots, d(A_m)^T \quad (16)$$

Where W is a non-fuzzy number.

C. *Aquifer vulnerability index (AVI) estimation:*

This involves the assignment of weights and rates to each groundwater conditioning factor. The aquifer vulnerability Index (VI) is the sum of the products of the assigned weight 'W' and ratings 'R' of all the factors used for the evaluation [73]. The technique used in estimating VI is termed the 'weighted linear average technique'. This technique is usually specified in terms of weightings (W) for each factor as well as rating score (R) for all options relative to each of the factors. The aquifer vulnerability Index (VI) equation is given in (17).

$$\mathrm{VI} = \sum w_i\ R_i \quad (17)$$

Where w_i is the weight (w) of parameter "i" and R is the rating score of parameter "i".

Equation (18) is the vulnerability index equation for each location estimated using the weights (W) and rating (R) of each factor,

$$VI = W_{HC}R_{HC} + W_{OLT}R_{OLT} + W_{OLR}R_{OLR} + W_{Li}\ R_{Li} + W_{Elev}\ R_{Elev} + W_{COA}\ R_{COA} \quad (18)$$

$$VI = 0.043R_{HC} + 0.091R_{OLT} + 0.249R_{OLR} + 0.514R_{Li} + 0.029R_E + 0.074R_{COA} \quad (19)$$

Where subscript HC, OLT, OLR, Li, Elev and COA, are the hydraulic conductivity, overlying layer thickness, overlying layer resistivity, lithology, elevation and coefficient of anisotropy weight and rating respectively (Table II).

D. *Validation of results:*

The primary objective of the validation is to check if the result from the FAHP prediction groundwater vulnerability model fits accurately with the study area. The validation was established by using Lead (Pb) - one of the chemical parameters considered from hydro-chemical analysis and longitudinal conductance - a geoelectric parameter across the study area. Both parameters were used to validate the generated vulnerability map using the FAHP model.

III. RESULT AND DISCUSSION

A. *VES Investigation Results:*

The summary of the interpreted VES results from the study area is as presented in Table II. The resistivity curves obtained based on the interpreted geo-electric data range from simple A, H, K (3-geoelectric layers), AA, AK, HA, KH, HK, QH, (4-geoelectric layers), and the complex 5-geoelectric layers (KHA, HKA, HKH, KHK). Field curves reflect the successive lithological sequence in any geologic environment and thus can be used qualitatively to assess the vulnerability of an area. The curve types from the study area can be classified into two (2) groups based on the confinement of the target aquifer(s). For Group 1, the curve types in this group include K, AK, KH, KHA and KHK where the aquifer layer(s) are overlaid by a confining layer. The aquifer layer in this group is well protected by the overlying layer [74]. For Group 2, the curve types in this group consist of A, AA, H, HA, HK, HKH, HAK, and QH. The aquifer layer(s) in this group are unconfined and thus the aquifer(s) are vulnerable.

Table II. Summary of Interpreted Results of the VES Curves

VES No.	Resistivity (ohm-m) $\rho_1/\ \rho_2/\ldots\ldots\rho_{n-1}/\ \rho_n$	Thickness (m) $h_1/\ h_2/\ldots\ h_{n-1}/\ h_n$	Depth (m) $Z_1/\ Z_2/\ \ldots.\ Z_{n-1}/\ Z_n$	Curve Type
1	101.6/121.3/51.1/462.5	1.3/6.4/11.2	1.3/7.7/18.9	KH
2	58.7/90.4/744.6	1.6/12.9	1.6/14.5	A
3	53.5/138.3/262.4	0.8/1.8	0.8/2.6	A
4	42.5/186.6/178.0/2729.6	0.9/17.6/3.2	0.9/18.5/21.7	KH
5	53.2/307.8/91.6/1760	0.9/6.1/8.4	0.9/7.0/15.4	KH
6	79.5/484.8/196.2/590.3	1.0/5.8/19.7	1.0/6.8/26.5	KH
7	72.0/154.7/33.1/144.2/1121.8	2.0/2.5/7.7/9.5	2.0/4.5/12.2/21.7	KHA
8	21.1/433.0/23.8/702.5	1.0/3.6/8.5	1.0/4.5/13.1	KH
9	47.1/105.9/152.5/585.6	1.0/9.8/2.2	1.0/10.8/13.0	HA
10	57.7/13.0/4712.5	1.5/ 2.4	1.5/3.9	H
11	271.9/161.8/1417.5	2.1/17.1	2.1/19.2	H
12	87.2/135.1/129.3/757.5	0.9/10.8/2.2	0.9/11.7/13.9	KH
13	92.9/261.5/40.2/528.0	0.8/2.7/13.5	0.8/3.5/17.0	KH
14	105.9/67.3/54.7/2536.0	4.1/5.6/1.2	4.1/9.7/10.9	QH
15	285.0/185.8/736.1	2.7/5.3	2.7/8.0	H
16	124.2/212.5/18.1/316.5	0.9/1.1/27.3	0.9/2.0/29.3	KH
17	92.1/171.5/92.7/364.9	0.8/6.3/3.2	0.8/7.1/10.3	KH
18	47.1/272.7/44.3/764.5	0.6/3.8/6.0	0.6/4.4/10.3	KH
19	76.4/182.7/40.7/991.7	0.9/3.2/10.4	0.9/4.1/14.5	KH
20	91.4/27.5/188.4	3.1/3.7	3.1/6.7	H
21	58.8/191.1/40.5/1321.0	0.8/2.6/8.6	0.8/3.4/12.0	KH
22	35.4/139.1/846.5	2.2/5.1	2.2/7.4	A
23	47.4/17.2/77.5/333.0	0.9/1.2/4.9	0.9/2.1/7.0	HA
24	75.0/63.8/704.6	1.2/18.5	1.2/19.7	H
25	47.7/22.1/76.6/1594.1	3.2/1.7/1.2	3.2/4.9/6.2	HA
26	91.4/184.2/246.0/1866.5	1.8/0.9/18.6	1.8/2.8/21.4	HA
27	71.7/141.1/1152.9	1.1/11.1	1.1/12.1	A
28	63.2/208.7/40.4/3455.4	0.9/2.2/6.7	0.9/3.1/9.8	KH
29	114.0/36.1/1471.9	1.7/12.6	1.7/14.3	H
30	72.8/165.9/1145.1/622.5	3.0/2.8/14.8	3.0/5.8/20.6	AK
31	107.5/31.2/199.0/1133.2	1.3/4.6/13.9	1.3/5.9/19.8	HA
32	55.3/200.1/1057.8	1.2/21.3	1.2/22.5	A
33	34.6/22.6/126.8/46.5	1.1/2.1/58.2	1.1/3.2/61.4	HK
34	27.1/296.3/406.3/1193.7	1.3/3.4/21.6	1.3/4.7/26.3	AA
35	10.4/292.9/7523.7	1.7/5.6	1.7/7.3	A
36	52.6/90.0/36.5/1093.6	1.0/2.4/10.1	1.0/3.4/13.5	KH
37	46.1/138.0/462.2/1136.6	1.1/4.0/13.5	1.1/5.1/18.6	AA
38	88.1/129.5/912.9	3.5/8.7	3.5/12.2	A
39	137.1/206.7/78.6/2446.7	1.6/6.0/8.1	1.6/7.6/15.7	KH
40	372.1/3409.9/2577.7	1.9/19.0	1.9/20.9	K
41	89.6/200.3/41.1/328.0	1.1/2.3/11.8	1.1/3.4/15.2	KH
42	16.2/3.4/136.0/189.9	0.5/1.4/12.3	0.5/1.9/14.2	HA
43	177.0/227.8/57.5/425.3	1.1/1.7/23.9	1.1/2.8/26.7	KH
44	98.4/116.0/51.5/182.8	1.6/3.4/17.3	1.6/5.0/22.4	KH
45	307.1/123.3/325.9/942.0	0.7/2.0/24.6	0.7/2.7/27.3	HA
46	790.1/206.7/425.0/657.6	0.5/1.7/51.5	0.5/2.2/53.6	HA
47	701.4/181.4/1780.3	0.5/19.7	0.5/20.1	H
48	85.5/100.7/712.0	3.3/10.1	3.3/13.4	A
49	109.4/99.5/401.4	1.2/7.1	1.2/8.2	H
50	65.9/42.4/153.5/789.1	1.0/1.6/15.6	1.0/2.6/18.2	HA
51	116.9/166.5/1324.4	1.8/11.5	1.8/13.2	A
52	160.4/260.2/2078.2	1.4/4.1	1.4/5.5	A
53	291.2/121.6/1596.3/695.5	0.9/2.3/12.6	0.9/3.3/15.8	HK
54	67.1/161.5/39.1/185.3	1.2/4.1/12.7	1.2/5.3/18.0	KH

55	172.9/17.9/114.8/844.5	0.4/1.3/23.9	0.4/1.7/25.6	HA
56	19.9/3.9/447.1	0.7/2.3	0.7/3.0	H
57	121.6/16.3/509.5	1.2/7.2	1.2/8.4	H
58	329.3/510.0/6.2/588.0	0.8/1.0/6.6	0.8/1.7/8.3	KH
59	83.1/21.5/125.5	1.8/9.4	1.8/11.2	H
60	137.0/231.0/29.0/716.0	0.9/2.6/10.2	0.9/3.5/13.7	KH
61	232.3/55.1/7033.3	0.8/3.1	0.8/3.9	H
62	180.6/335.3/94.0/438.8	2.0/3.4/3.8	2.0/5.4/9.2	KH
63	148.6/52.7/750.2/2830.0	0.8/1.6/3.1	0.8/2.4/5.5	HA
64	46.3/11.6/345.3	1.2/2.5	1.2/3.7	H
65	171.0/94.5/804.6/2105.4	1.0/1.7/33.9	1.0/2.7/36.6	HA
66	96.3/178.4/25.9/365.6	0.7/1.9/18.1	0.7/2.6/20.7	KH
67	247.8/542.6/92.4/509.3/84.1	0.6/1.0/4.3/17.8	0.6/1.6/5.9/23.7	KHK
68	213.2/420.4/14.4/886.4	0.6/0.8/5.3	0.6/1.4/6.7	KH
69	113.3/8.7/67.5/479.1	0.8/7.0/14.9	0.8/7.8/22.8	HA
70	382.9/77.2/21.7/370.5	0.7/2.1/9.5	0.7/2.8/12.3	QH
71	22.2/25.8/503.3	1.2/15.3	1.2/16.5	A
72	78.5/120.2/23.6/521.4	0.8/1.7/7.6	0.8/2.5/10.1	KH
73	189.1/280.9/2597.8/140.5	1.1/4.5/14.2	1.1/5.6/19.9	AK
74	105.6/46.8/1900.2/1440.9	0.7/1.3/7.7	0.7/2.1/9.8	HK
75	82.4/8.6/37.1/558.1	0.6/1.5/18.0	0.6/2.1/20.1	HA
76	13.1/134.3/617.1	3.0/9.7	3.0/12.7	A
77	68.0/30.0/112.4/435.0	0.8/2.3/24.4	0.8/3.1/27.4	HA
78	66.8/13.4/106.9/181.5	1.4/ 3.5/32.9	1.4/4.9/37.8	HA
79	60.2/160.7/33.0/642.6	0.6/1.7/5.3	0.6/2.3/7.6	KH
80	146.8/48.9/873.3	1.0/23.0	1.0/24.0	H
-	---	---	---	---
-	---	---	---	---
-	---	---	---	---
173	77.5/565.4/25.8/358.4	0.9/2.6/11.6	0.9/3.5/15.1	KH
174	77.6/457.9/15.8/359.9	0.9/2.6/14.2	0.9/3.5/17.7	KH
175	59.0/49.0/207.0	4.1/3.5	4.1/7.6	H
176	97.2/15.1/233.5	2.6/3.3	2.6/5.9	H
177	90.3/51.7/601.1	0.8/13.2	0.8/14.0	H
178	40.0/184.0/16.0/471.0	1.1/3.2/9.8	1.1/4.3/14.1	KH
179	40.0/98.0/11.0/307.0	1.0/2.0/6.0	1.0/3.0/9.0	KH
180	551.1/187.9/560.0	1.1/39.8	1.1/40.9	H
181	294.3/299.6/38.0	3.1/8.9	3.1/12.0	K
182	59.7/195.6/28.4	0.5/3.8	0.5/4.3	K
183	158.2/350.7/102.1/465.0	1.0/3.2/12.8	1.0/4.2/17.0	KH
184	114.7/27.3/1159.4	1.1/8.8	1.1/9.9	H
185	425.5/738.5/36.4/610.3	0.8/1.3/12.2	0.8/2.1/14.3	KH
186	70.4/446.0/49.9	1.7/2.5	1.7/4.2	K
187	43.5/562.4/21.3/389.1	0.9/2.4/11.2	0.9/3.3/14.5	KH

B. Elevation (Elev):

The elevation map (Fig. 6) reveals that the study area is moderately undulating with surface elevation ranging from 330 - 388 m. During precipitation, the surface water flows from northwestern - southeastern direction. The higher the elevation, the lower the infiltration while the lower the elevation, the higher the infiltration. High infiltration increases the vulnerability of groundwater while low infiltration reduces the vulnerability of groundwater. The produced thematic map shows that the southern region of the study area which has a very low elevation of 330 - 356 m is more vulnerable. Low elevation falls within the class of 357 - 361 m in the southeastern and central regions which is vulnerable. The northeastern and northwestern region of the study area shows a moderate elevation of 362 - 365 m which is moderately less vulnerable, while high elevation falls within the class greater than 366 m will be less vulnerable. This is evident in the northeastern and northwestern parts of the study area.

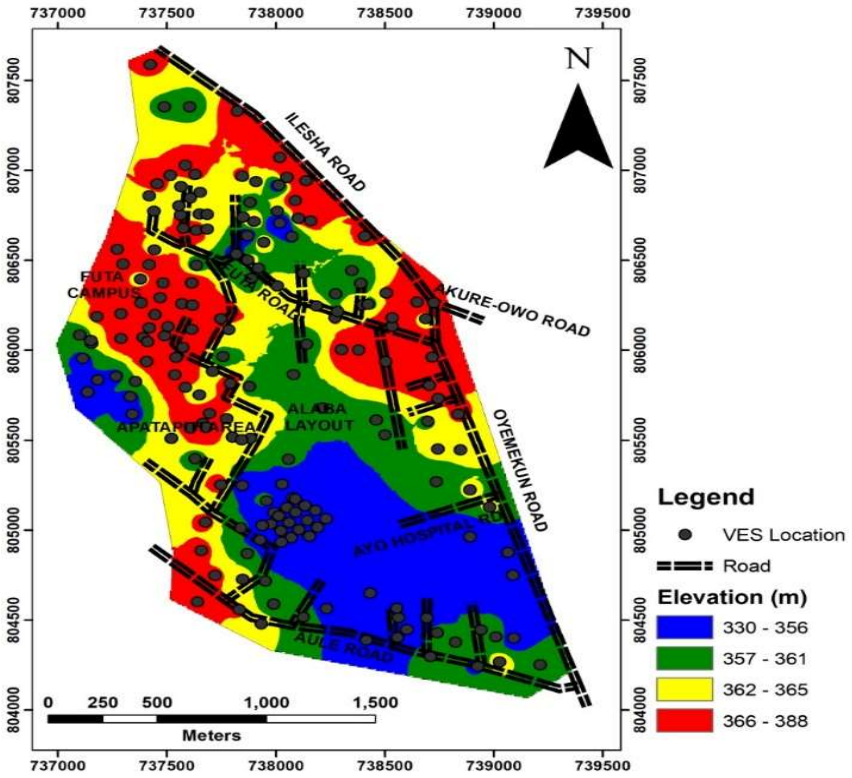

Fig. 6 Elevation Map of the Study Area

C. Lithology (Li):

Four rock types were identified in the study area: quartzite, granite, porphyritic granite and charnockite. The geological map of the study area (refer to Fig. 2) shows that charnockitic rocks cover a larger area than the other rocks. The charnockitic areas could be associated with low vulnerability because it weathers essentially into clay which has high porosity but low permeability. A smaller portion of the study area underlain by quartzite rocks is associated with high vulnerability since the weathering product of quartzite has higher porosity and permeability than charnockite as it tends to weather into sand. Part of the area underlain by granite and porphyritic granite is considered to be of moderate vulnerability.

D. Overlying Layer Resistivity (OLR):

The overlying layer resistivity map (Fig. 7) is the iso-resistivity map of the layer overlying the aquifer layer across the study area. The spatial variation of the OLR in the study area was grouped into four zones (very low, low, moderate and high) ranging from (4.977 - 69.69, 69.7 - 100.5, 100.6 - 140.6 and 140.7 - 790.8 Ω-m) respectively. The OLR map shows that the overburdened material in the study area is characterized by very low to low resistivity values at the northern, southern, northeastern and pockets of the central parts of the study area. This is an indication that these parts of the study area will have good protective capacity and that the aquifer in these sections is less vulnerable to contaminants. The northwestern, southwestern, southeastern and northeastern parts of the area correspond to the zones with moderate to high aquifer resistivity. This is an indication that these portions will exhibit moderate protective capacity and aquifers in these sections will be more vulnerable.

E. Overlying Layer Thickness (OLT):

The overlying layer thickness map of the area (Fig. 8) is the isopach of the layer(s) overlying the aquifer layer across the area. The thickness of the overlying layer ranges from 0.42 to 23 m. The OLT map shows that the aquifer overlying material in the study area is generally thin (generally less than 10m) at the enclosed part of the northern, southern, northwestern and eastern parts of the study area, this implies that the aquifers in these areas are highly vulnerable. The OLT in the northeastern and southwestern part of the study area is moderate to highly thick (> 20 m). The thicker the overlying layer, the less vulnerable the aquifer layer. Given the general thin nature of the overlying layer, infiltration of potential contaminants from the surface to the aquifer unit will be short and the underlying aquifer units can be easily contaminated.

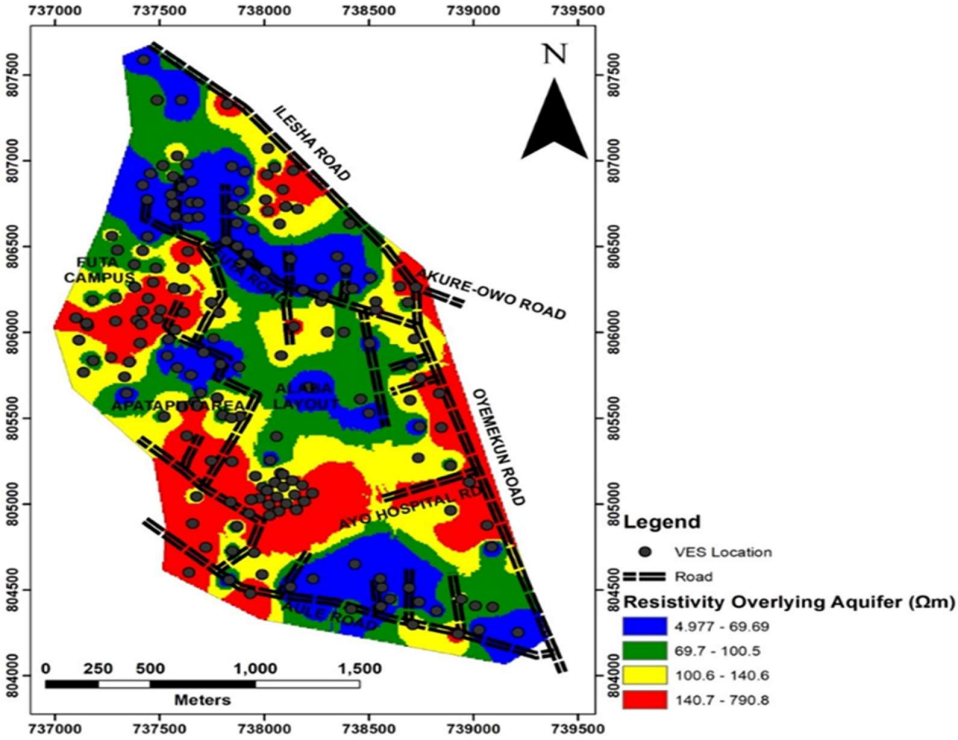

Fig. 7 Overlying Layer Resistivity Map of the Study Area

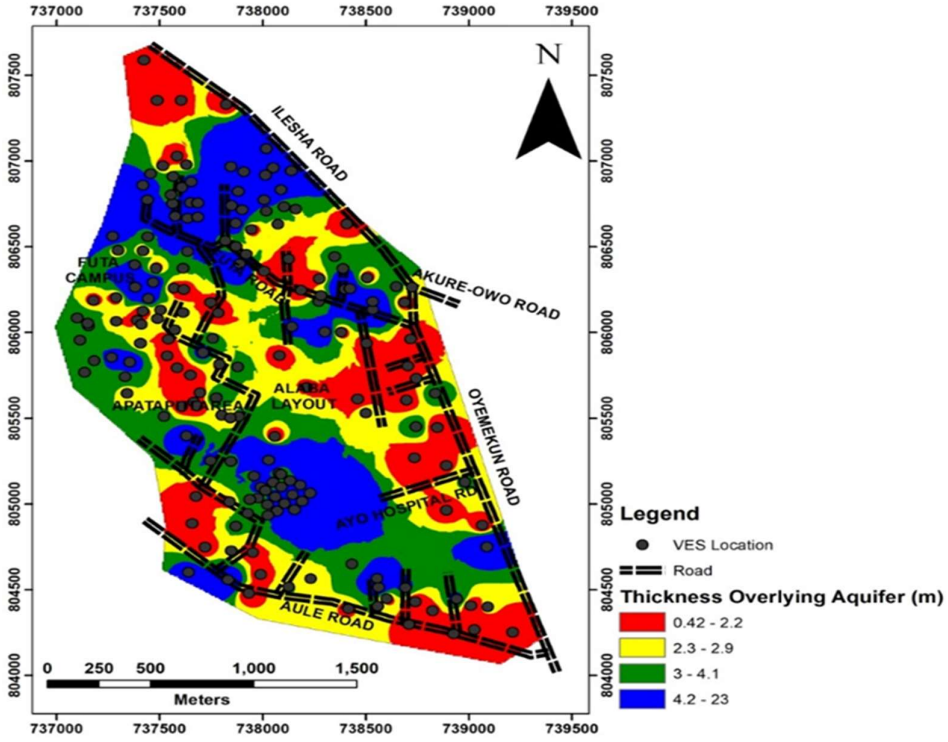

Fig. 8 Overlying Layer Thickness Map of the Study Area.

F. Hydraulic Conductivity (K):

The hydraulic conductivity (k) distribution in the area ranges from 0.000037 - 0.052 m/day (Fig. 9). The hydraulic conductivity determines the ease at which contaminants will infiltrate the aquifer layer. Areas of high hydraulic conductivity are usually made up of geologic formations with low protective capacity and are vulnerable to pollution. The hydraulic conductivity map shows that the study area is dominated by very low to low hydraulic conductivity values. Moderate to high hydraulic conductivity is evident in the northeastern, southeastern, and southwestern parts of the study area.

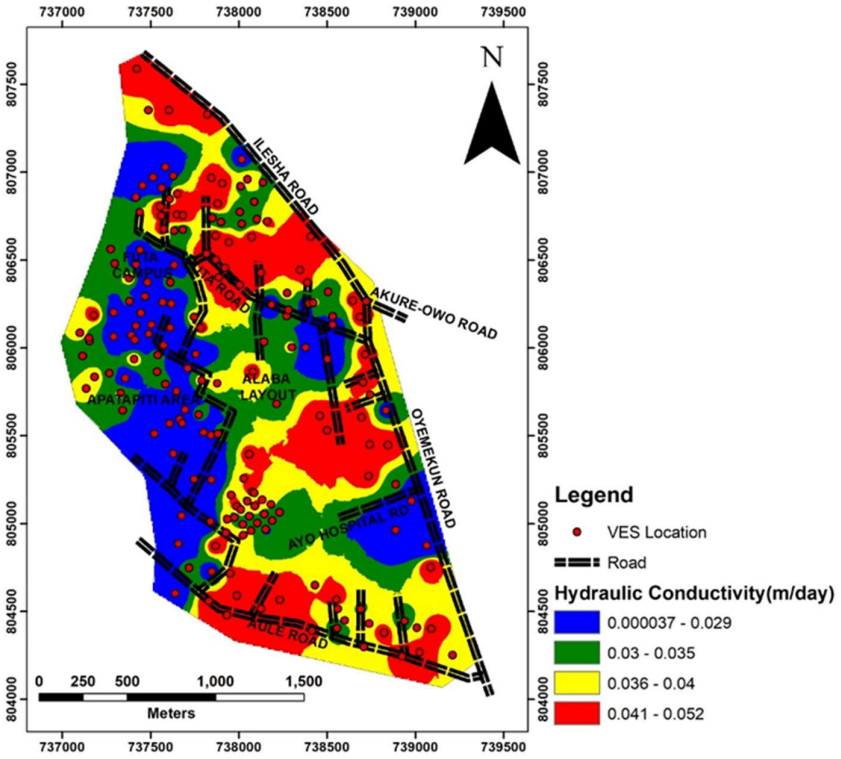

Fig. 9 Overlying Layer Thickness Map of the Study Area.

Table III. Summary of the Vulnerability Assessment Parameters

VES Points	Easting	Northing	Elev	Li	OLR	OLT	COA	K
1	737273	806562	367	Qtz	117.455	7.7	0.008514	0.002374
2	737297	806481	368	Qtz	58.7	1.6	0.017036	0.003624
3	737418	806477	372	Qtz	138.3	1.8	0.007231	0.002043
4	737482	806375	365	Qtz	42.5	0.9	0.023529	0.004072
5	737469	806293	388	Qtz	190.5521	7	0.005248	0.001402
6	737445	806200	371	Qtz	277.0725	6.8	0.003609	0.000752
7	737380	806266	363	Qtz	44.11236	12.2	0.022669	0.004025
8	737379	806396	360	Qtz	82.57423	4.6	0.01211	0.003052
9	737290	806204	369	Qtz	47.1	1	0.021231	0.00394
10	737179	806187	366	Qtz	57.7	1.5	0.017331	0.00365
-	-	-	-	-	-	-	-	-
-	-	-	-	-	-	-	-	-
180	739065	804876	353	Ch	551.1	1.1	0.001815	0.000105
181	738980	805129	362	Ch	294.3	3.1	0.003398	0.000664
182	738186	806247	362	Ch	59.7	0.5	0.01675	0.003598
183	738836	805645	366	Ch	271.92	4.2	0.003678	0.000781
184	738717	805963	367	Ch	114.7	1.1	0.008718	0.002421
185	738724	806266	378	Ch	577	2.1	0.001733	8.68E-05
186	738017	807073	373	Ch	141.2	4.2	0.007082	0.002001
187	738049	806961	371	Ch	26.33	14.5	0.037979	0.004575

G. Coefficient of Anisotropy (K)

Fig. 10 depicts the coefficient of Anisotropy map of the study area. The study area is characterized by a coefficient of anisotropy (λ) ranging from 1 - 3.51 (Table III). The eastern and southwestern flank is characterized by high anisotropy coefficient values, and the south and northwest flank exhibits a low anisotropy coefficient. The high value of the coefficient of anisotropy suggests that the fracture system must have extended in all directions with different degrees of fracturing; this may allow easy passage of water either polluted or unpolluted. On the other hand, a low coefficient of anisotropy may arise from unidirectional fracture, which may not allow an easy flow of water. Therefore, high values of the coefficient of anisotropy suggest high vulnerability of the underlying aquifer to polluting fluid and vice versa [8, 36].

H. Application of the developed FAHP in Aquifer vulnerability index (AVI) estimation:

The generated AVCF maps were used to classify and rate the vulnerability factors with the aid of the FAHP model using Chang's extent analysis method. The scale for pairwise comparisons prepared for the six parameters considered for groundwater vulnerability conditioning factors of one attribute over another in the fuzzy AHP method in the study area is presented in Table IV using [70] 2008 scale. The total weights of all the criteria must be normalized to 1; therefore, the obtained fuzzy calculations were normalized to obtain the weight value of 1. The basic components of the developed FAHP are the normalized weight (W) and the rating (R) for the AVCFs' parameters (Table V). Ratings of 1 - 5 were given to each of the parameters within the factors influencing the aquifer vulnerability of the study area. The ratings will assist in the estimation of the aquifer vulnerability index of the area. The results show that lithology has the highest FAHP weightage of 0.3264 and the elevation with the lowest weight of 0.0340.

I. Aquifer Vulnerability (Model) Map:

The computed AVI values were processed in the GIS environment. Equations (17), (18), and (19) were applied in the computation of vulnerability index value involving multi-criteria synthesis of the produced AVCFS maps. The estimated VI values vary between 1.0494 and 4.4599 (Table VI). The aquifer vulnerability (model) map (Fig. 11) was produced using the ArcGIS 10.3 software. The aquifer vulnerability map has categorized the study area into four zones by adopting the Natural Breaks Approach [75], namely: very low, low, moderate and high aquifer vulnerability zones using the Quantile Classification Techniques. The very low to low vulnerable zones were observed in the northern and southern part of the study area (charnockitic rock type), and the high to very highly vulnerable zones (poor aquifer protective capacity) is widespread in the eastern and eastern part of the map since the rock type in the area is quartzite.

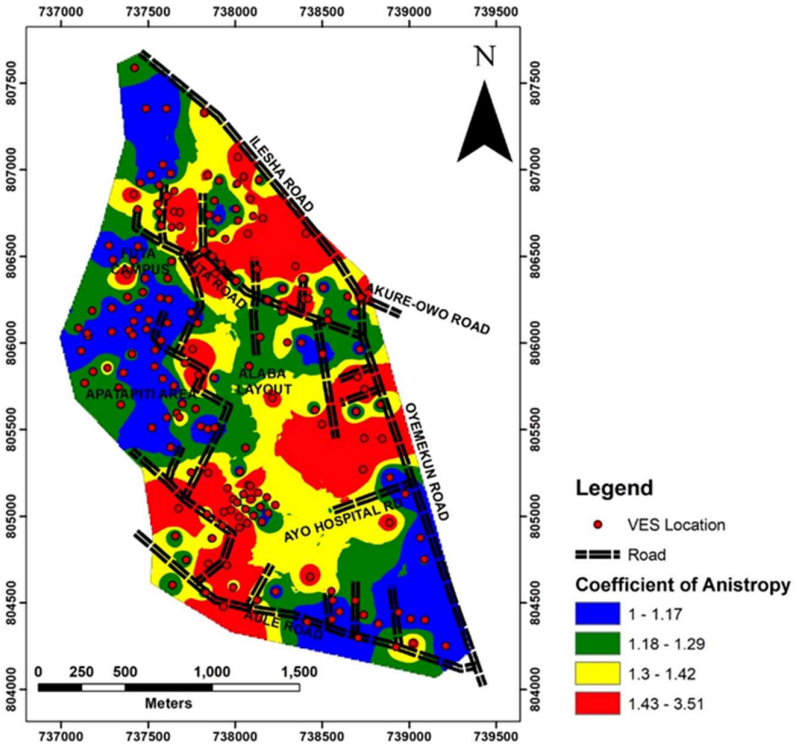

Fig. 10 Coefficient of Anisotropy Map of the Study Area.

Table IV. Comparison matrix of the parameters

Criteria	Hydraulic Conductivity	Overlying Layer Thickness	Overlying Layer Resistivity	Lithology	Elevation	Coefficient of Anisotropy
Hydraulic Conductivity	(1, 1, 1)	(½, 2/3, 1)	(2/5, ½, 2/3)	(1/3, 2/5, ½)	(½, 1, 2)	(2/3, 1, 2)
Overlying Layer Thickness	(1, 3/2, 2)	(1, 1, 1)	(½, 2/3, 1)	(½, 2/3, 1)	(3/2, 2, 5/2)	(½, 1, 3/2)
Overlying Layer Resistivity	(3/2, 2, 5/2)	(1, 3/2, 2)	(1, 1, 1)	(½, 2/3, 1)	(3/2, 2, 5/2)	(1, 3/2, 2)
Lithology	(2, 5/2, 3)	(1, 3/2, 2)	(1, 3/2, 2)	(1, 1, 1)	(3/2, 2, 5/2)	(5/2, 3, 7/2)
Elevation	(½, 1, 2)	(2/5, ½, 2/3)	(2/5, ½, 2/3)	(2/7, 1/3, 2/5)	(1, 1, 1)	(½, 2/3, 1)
Coefficient of Anisotropy	(½, 1, 3/2)	(2/3, 1, 2)	(½, 2/3, 1)	(2/5, ½, 2/3)	(1, 3/2, 2)	(1, 1, 1)

Table V. Ratings for classes of factors

Influencing Factors	Classes	Pollution potentiality for groundwater vulnerability	Rating (Unstandardized Values)	Normalized Weight (W)
Hydraulic Conductivity (K)	0.0000366 - 0.0292	Very low	1	0.0932
	0.0293 - 0.0355	Low	2	
	0.0356 - 0.0399	Moderate	3	
	0.04 - 0.052	High	5	
Overlying Layer Thickness (OLT)	0.42 - 2.2	High	5	0.1720
	2.3 - 2.9	Moderate	3	
	3 - 4.1	Low	2	
	4.2 – 23	Very Low	1	
Overlying Layer Resistivity (OLR)	4.977 - 69.69	Very Low	1	0.2397
	69.7 - 100.5	Low	2	
	100.6 - 140.63	Moderate	3	
	140.7 - 790.8	High	5	
Lithology (L)	Quartzite	High	5	0.3264
	Granite	Moderate	3	
	Porphyritic granite	Moderate	3	
	Charnockite	Low	2	
Elevation (Elev)	330 - 356	Very Low	5	0.0340
	357 - 361	Low	3	
	362 - 365	Moderate	2	
	366 – 388	High	1	
Coefficient of Anisotropy (COA)	1 - 1.17	Very Low	1	0.1347
	1.18 - 1.29	Low	2	
	1.3 - 1.42	Moderate	3	
	1.43 - 3.51	High	5	

Table VI. Vulnerability index estimation for all the VES stations

VES points	Location		Elev (0.034)		OLT (0.172)		OLR (0.2397)		K (0.0932)		COA (0.1347)		Li (0.3264)		VI
	Easting	Northing	R	W*R	R	W*R	R	W*R	R	W*R	R	W*R	R	W*R	$\sum(W \times R)$
1	737273	806562	1	0.034	1	0.172	3	0.7191	2	0.1864	1	0.1347	5	1.632	2.8782
2	737297	806481	1	0.034	5	0.86	1	0.2397	1	0.0932	1	0.1347	5	1.632	2.9936
3	737418	806477	1	0.034	5	0.86	3	0.7191	1	0.0932	1	0.1347	5	1.632	3.473
4	737482	806375	2	0.068	5	0.86	1	0.2397	1	0.0932	1	0.1347	5	1.632	3.0276
5	737469	806293	1	0.034	1	0.172	5	1.1985	1	0.0932	2	0.2694	5	1.632	3.3991
6	737445	806200	1	0.034	1	0.172	5	1.1985	1	0.0932	1	0.1347	5	1.632	3.2644
7	737380	806266	1	0.034	1	0.172	1	0.2397	2	0.1864	2	0.2694	5	1.632	2.5335
8	737379	806396	1	0.034	1	0.172	2	0.4794	5	0.466	5	0.6735	5	1.632	3.4569
9	737290	806204	1	0.034	5	0.86	1	0.2397	1	0.0932	1	0.1347	5	1.632	2.9936
10	737179	806187	1	0.034	5	0.86	1	0.2397	5	0.466	2	0.2694	5	1.632	3.5011
11	737290	806065	1	0.034	5	0.86	5	1.1985	1	0.0932	1	0.1347	5	1.632	3.9524
12	737391	806073	2	0.068	5	0.86	2	0.4794	1	0.0932	1	0.1347	5	1.632	3.2673
13	737099	806086	3	0.102	2	0.344	5	1.1985	3	0.2796	2	0.2694	2	0.6528	2.8463
14	737114	805955	5	0.1264	2	0.344	3	0.7191	2	0.1864	1	0.1347	2	0.6528	2.207
15	737490	806080	1	0.034	3	0.516	5	1.1985	1	0.0932	1	0.1347	2	0.6528	2.6292
16	737407	805938	1	0.034	5	0.86	5	1.1985	5	0.466	2	0.2694	5	1.632	4.4599
17	737356	805829	2	0.068	1	0.172	5	1.1985	1	0.0932	1	0.1347	5	1.632	3.2984
18	737267	805856	5	0.17	1	0.172	5	1.1985	2	0.1864	2	0.2694	2	0.6528	2.7838
19	737135	805769	5	0.17	2	0.344	5	1.1985	3	0.2796	2	0.2694	2	0.6528	2.9143
20	737182	805836	5	0.17	2	0.344	1	0.2397	5	0.466	2	0.2694	2	0.6528	2.1419
21	737331	805742	5	0.17	2	0.344	3	0.7191	3	0.2796	2	0.2694	2	0.6528	2.4349
22	737342	805645	5	0.17	5	0.86	1	0.2397	2	0.1864	1	0.1347	2	0.6528	2.3783
23	737536	805864	1	0.034	5	0.86	1	0.2397	2	0.1864	1	0.1347	5	1.632	3.0868
24	737584	805794	2	0.068	5	0.86	2	0.4794	2	0.1864	1	0.1347	5	1.632	3.3605
25	737542	805960	1	0.034	5	0.86	1	0.2397	3	0.2796	1	0.1347	2	0.6528	2.2008
26	737612	806116	1	0.034	3	0.516	3	0.7191	1	0.0932	1	0.1347	2	0.6528	2.1498
27	737568	806261	1	0.034	5	0.4509	2	0.479	1	0.0932	5	0.6735	2	0.6528	2.2541
28	737612	806375	1	0.034	3	0.516	3	0.7191	3	0.2796	2	0.2694	2	0.6528	2.4079
29	737746	806176	1	0.034	5	0.86	3	0.7191	3	0.2796	1	0.1347	2	0.6528	2.6802
30	737756	805965	5	0.17	2	0.344	2	0.4794	1	0.0932	5	0.6735	2	0.6528	2.4129
-	-	-		-		-		-		-		-		-	-
-	-	-		-		-		-		-		-		-	-
-	-	-		-		-		-		-		-		-	-
180	739065	804876	5	0.17	5	0.86	5	1.1985	1	0.0932	1	0.1347	2	0.6528	3.1092
181	738980	805129	2	0.068	2	0.344	5	1.1985	1	0.0932	1	0.1347	2	0.6528	2.4912
182	738186	806247	2	0.068	5	0.86	1	0.2397	1	0.0932	1	0.1347	2	0.6528	2.0484
183	738836	805645	1	0.034	1	0.172	5	1.1985	1	0.0932	1	0.1347	2	0.6528	2.2852
184	738717	805963	1	0.034	5	0.86	3	0.7191	5	0.466	1	0.1347	2	0.6528	2.8666
185	738724	806266	1	0.034	5	0.86	5	1.1985	3	0.2796	5	0.6735	2	0.6528	3.6984
186	738017	807073	1	0.034	1	0.172	5	1.1985	1	0.0932	5	0.6735	2	0.6528	2.824
187	738049	806961	1	0.034	1	0.172	1	0.2397	5	0.466	5	0.6735	2	0.6528	2.238

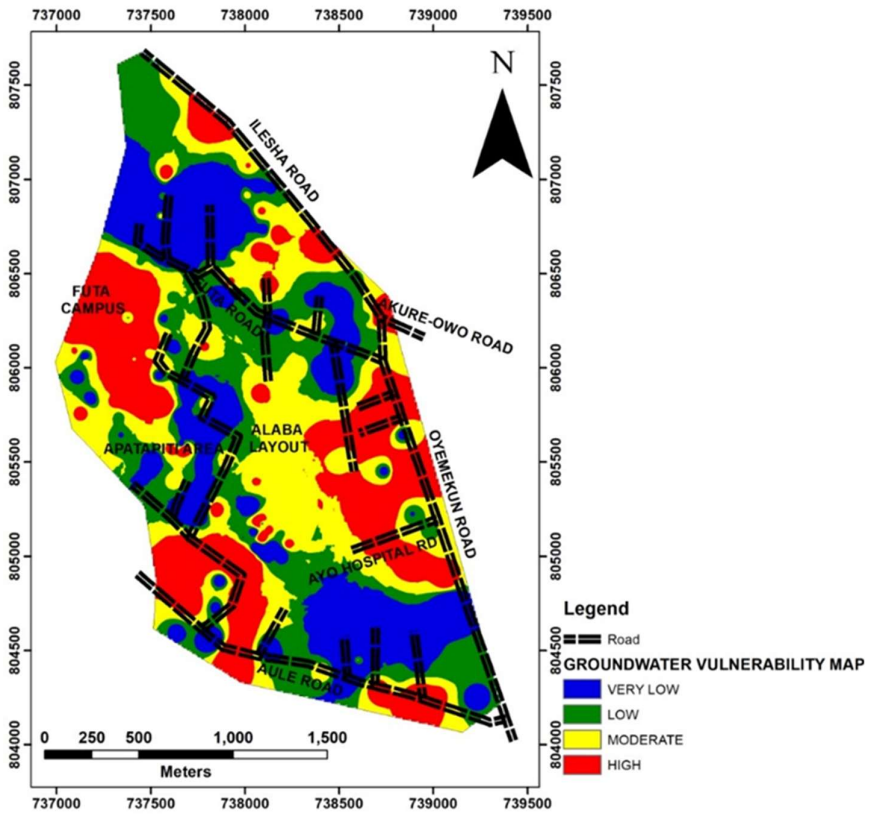

Fig. 11 Aquifer Vulnerability Map.

J. Validation of the groundwater vulnerability model:

Validation was conducted to ascertain the accuracy of the produced aquifer vulnerability model map. This was done by carrying out chemical analysis on 15 water samples obtained from wells across the area (see Fig. 5). The samples were analyzed to determine their physico-chemical properties. The physiochemical properties include pH, Conductivity, temperature, turbidity, TDS, hardness, nitrate (NO_3^-), calcium (Ca^{2+}), sulphate (SO_4^{2-}), chloride (Cl^-), magnesium (Mg^{2+}), manganese (Mn^{2+}), zinc (Zn), cadmium (Cd), chromium (Cr), nickel (Ni) and lead (Pb). Zinc, cadmium, chromium lead and nickel are mostly the heavy metals found in the mechanic workshop waste that can pose health hazards to humans and the environment [76]. Their concentration levels were stated in relation to World Health Organization [77] permissible levels (Table VII).

The concentration levels of all the parameters revealed that the concentration analysis falls within the permissible limit. However, the heavy metal analysis result shows that Cr, Cd and Pb concentration values are close to the upper limit (SON standard) and relatively high above the permissible level (Table VII). Lead (Pb) is one of the hydrocarbon properties which were observed within the permissible limits in some samples and exceeding permissible limits in others. Pb was selected for the validation of the model developed for vulnerability assessment in the study area because it is one of the by-products of hydrocarbon and it can serve as an index element of hydrocarbon pollution. (Fig. 12). The classes of the groundwater vulnerability zones were compared with that of the lead concentration, which was produced in the GIS environment to ascertain its success rate accuracy. This was done to identify the numbers of well samples that coincided/did not coincide with vulnerability (Table VIII). For a more reliable result, the prediction of vulnerable zones of the model map was validated using longitudinal conductance (Fig. 13).

The validation map was produced by posting the longitudinal conductance (LC) values on the groundwater vulnerability model map (FAHP). The map was validated using visual inspection, this helps to indicate areas where the LC and vulnerability map coincide. The longitudinal conductance provides a measure of the aquifer-protected capacity of a particular layer [78]. The validation result is presented in Table IX.

The percentage accuracy calculation for the FAHP prediction model map based on the Lead parameter can be obtained as follows:

Total number of well samples analyzed = 15

Number of wells where the vulnerability coincides = 11

Number of wells where the vulnerability does not coincide = 4

$$Success\ rate\ (accuracy)\ of\ the\ prediction = \frac{11}{15} \times 100 = 73\%$$

On this basis, the conceptual model gives an accuracy of 73% which is reliable and considerable for a good prediction.

The percentage accuracy calculation for the FAHP prediction model map based on longitudinal conductance can be obtained as follows:

Total number of well samples analyzed = 186

Number of 'LC' where the vulnerability coincides = 138

Number of 'LC' where the vulnerability does not coincide = 48

$$Success\ rate\ (accuracy)\ of\ the\ prediction = \frac{138}{186} \times 100 = 74\%$$

On this basis, the conceptual model gives an accuracy of 74% which is reliable and considerable for a good prediction.

From these results, the correlation of the FAHP model based on lead is 73% and longitudinal conductance is 74%. This confirmed that both results are reliable.

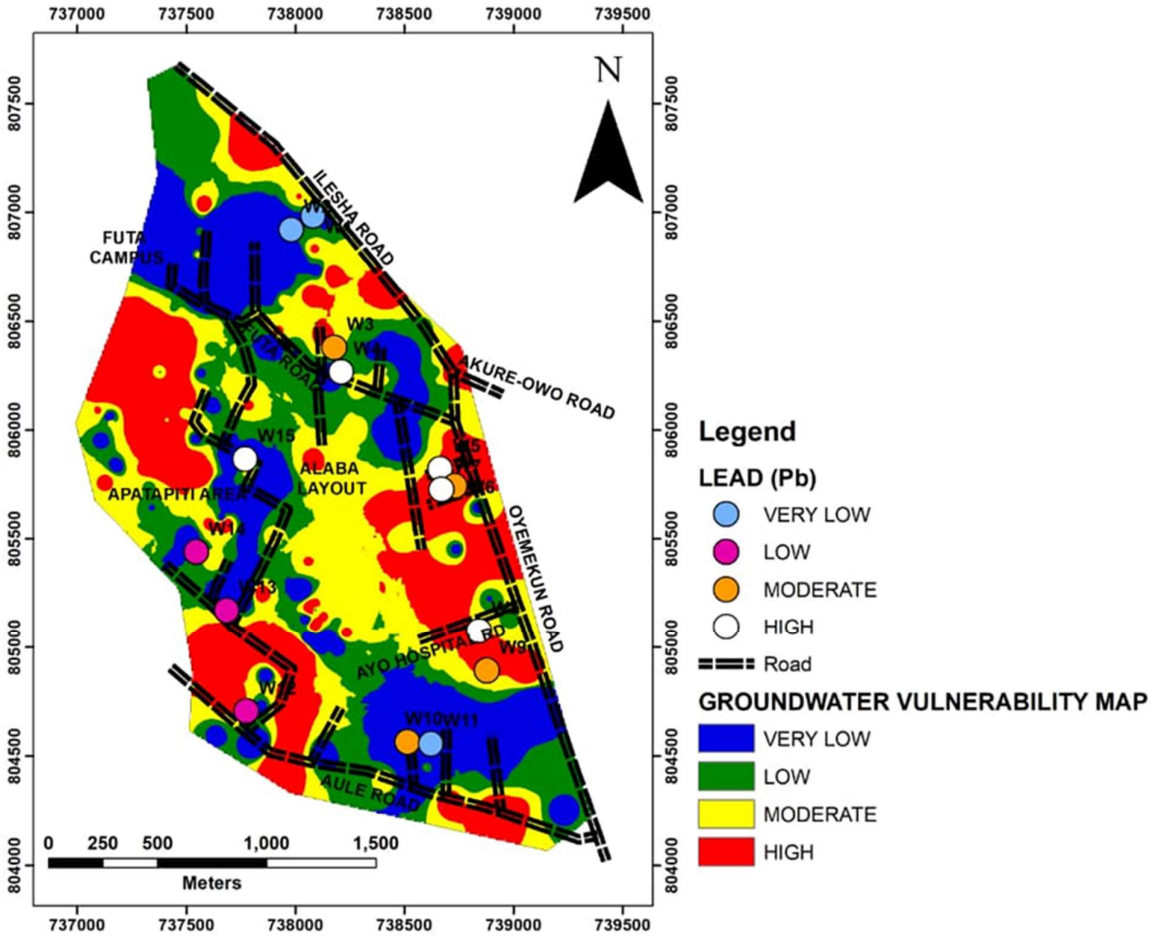

Fig. 12 Validation Map of the Study Area (Lead).

Table VII. Results of the Hydro-physicochemical Analysis of Water Samples in the Study Area

Sample No	1	2	3	4	5	6	7	8	9	10	11	12	13	14	15	WHO Standard
Temperature (0℃)	32.12	30.23	26.94	20.29	20.42	26.94	30.23	29.15	29.38	29.53	29.14	26.75	29.56	28.62	28.51	NA
PH	6.54	6.06	6.54	6.35	6.52	5.89	5.64	5.92	5.79	5.61	6.10	6.08	6.59	5.72	5.79	6.5-8.5
Total dissolved solids (mg/L)	93	129	203	105	100	93	94	96	117	187	156	132	164	188	137	500
Conductivity (μS/cm)	185	259	405	215	202	186	187	192	235	374	312	262	328	376	269	1000
Salinity	0.08	0.12	0.20	0.10	0.10	0.11	0.16	0.09	0.11	0.17	0.14	0.12	0.15	0.17	0.12	
Turbidity (NTU)	4.25	4.87	0.85	0.05	0.00	0.85	3.5	0.02	0.85	1.65	0.01	0.00	2.12	0.00	0.05	5NTU
Dissolved oxygen	8.26	3.63	4.53	4.32	5.05	9.27	5.85	2.78	2.53	2.41	2.38	2.49	2.34	2.21	2.21	
Total hardness (mg/l)	72	80	76	94	90	67	70	88	45	70	90	68	74	82	70	100
Nitrate (mg/l)	0.20	0.50	1.00	0.25	0.80	0.70	0.20	1.00	0.25	0.60	0.30	0.50	0.25	0.30	1.00	50
Magnesium (mg/l)	15	25	30	18.5	23	35	16.8	8	20.6	15.2	14	28.5	16	18	30	30
Sulphate (mg/l)	50	67	80	144	198	145	168	123	194	80	144	165	120	196	123	200-250
Chloride (mg/l)	25	28	22	26	21	20	24	29	22	21	24	27	28	22	27	200-250
Manganese (mg/l)	0.1	0.05	0.12	0.05	0.2	0.05	0.15	0.15	0.01	0.01	0.1	0.2	0.1	0.05	0.1	0.1
Calcium (mg/l)	35	50	55	39	72	45	42	38	70	72	32	55	72	68	65	75
Lead (Pb)	0.01	0.016	0.004	0.009	0.008	0.005	0.006	0.006	0.0045	0.003	ND	ND	ND	ND	0.026	0.01
Chromium (Cr)	0.049	0.053	0.045	0.038	0.033	0.039	0.021	0.024	0.029	0.031	0.03	0.025	0.022	0.031	0.025	0.05
Cadmium (Cd)	ND	ND	ND	0.0009	ND	ND	ND	ND	ND	ND	0.00114	ND	0.00172	ND	0.0031	0.003
Nickel (Ni)	ND	ND	ND	ND	ND	ND	ND	ND	ND	ND	ND	ND	ND	ND	ND	0.07
Zinc (Zn)	ND	ND	ND	ND	ND	ND	ND	ND	ND	ND	ND	ND	ND	ND	ND	0.03

Table VIII. Water Analysis - (Pb) Validation

S/N	Eastings	Northings	Lead (Pb)	Pb Rating	Groundwater Vulnerability Rating	Remark
1	738081	806985	0.01	Very Low	Very Low	Coincide
2	737982	806922	0.016	Very Low	Very Low	Coincide
3	738178	806380	0.004	Moderate	Moderate	Coincide
4	738211	806268	0.009	High	Low	Not Coincide
5	738664	805822	0.008	High	High	Coincide
6	738732	805744	0.005	High	High	Coincide
7	738669	805727	0.006	Moderate- High	High	Coincide
8	738842	805076	0.006	High	High	Coincide
9	738878	804892	0.0045	Moderate	Moderate	Coincide
10	738514	804565	0.003	Moderate	Low	Not Coincide
11	738622	804557	ND	Very Low	Very Low	Coincide
12	737775	804706	ND	Low	High	Not Coincide
13	737686	805172	ND	Low	Low	Coincide
14	737546	805441	ND	Very Low- Low	Very Low	Coincide
15	737770	805868	0.026	High	Low	Not Coincide

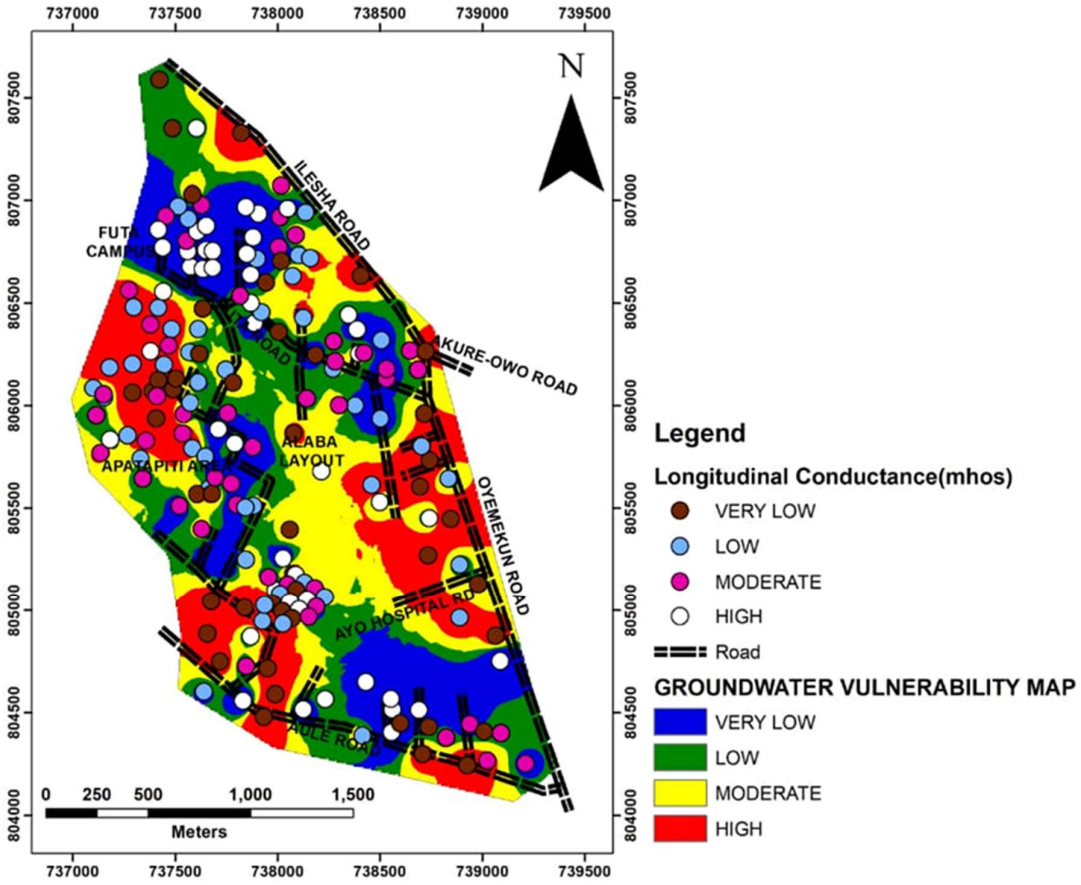

Fig. 13 Validation Map of the Study Area (Longitudinal Conductance).

Table IX. Validation results for the groundwater vulnerability (Longitudinal Conductance)

VES No	Easting	Northing	Longitudinal conductance (mhos)	Longitudinal Conductance Rating	Groundwater Vulnerability (FAHP) Rating	Remark
1	737273	806562	0.065557	Moderate - High	High	Not coincide
2	737297	806481	0.027257	Very low - Low	High	coincide
3	737418	806477	0.013015	Very low - Low	High	Coincide
4	737482	806375	0.021176	Very low - Low	High	Coincide
5	737469	806293	0.036735	Very low - Low	High	coincide
6	737445	806200	0.024542	Very low - Low	High	Coincide
7	737380	806266	0.276566	Moderate - High	High	Not Coincide
8	737379	806396	0.055707	Very low - Low	High	coincide
9	737290	806204	0.021231	Very low - Low	High	Coincide
10	737179	806187	0.025997	Very low - Low	High	Coincide
11	737290	806065	0.007746	Very low - Low	High	coincide
12	737391	806073	0.010321	Very low - Low	High	coincide

13	737099	806086	0.018936	Very low - Low	High	coincide
14	737114	805955	0.038716	Very low - Low	High	Coincide
15	737490	806080	0.009474	Very low - Low	High	Coincide
16	737407	805938	0.012423	Very low- Low	High	Coincide
17	737356	805829	0.045421	Very low - Low	High	Coincide
18	737267	805856	0.026674	Very low - Low	High	Coincide
19	737135	805769	0.029295	Very low - Low	High	Coincide
20	737182	805836	0.134545	Moderate - High	Low	Coincide
21	737331	805742	0.027211	Very low - Low	Very low	Not Coincide
22	737342	805645	0.062147	Moderate - High	Low	Coincide
23	737536	805864	0.069767	Moderate - High	High	Not coincide
24	737584	805794	0.016	Very low - Low	High	Coincide
25	737542	805960	0.076923	Moderate - High	High	Not coincide
26	737612	806116	0.02458	Very low - Low	Low	Not coincide
27	737568	806261	0.015342	Very low - Low	High	Coincide
28	737612	806375	0.024782	Very low - Low	High	Coincide
29	737746	806176	0.014912	Very low - Low	Very Low	Not Coincide
30	737756	805965	0.041209	Very low - Low	High	Coincide
-			-	-	-	-
-			-	-	-	-
180	739065	804876	0.001996	Very low – Low	High	Coincide
181	738980	805129	0.010533	Very low – Low	Very Low	Not Coincide
182	738186	806247	0.008375	Very low – Low	Very Low	Not Coincide
183	738836	805645	0.015446	Very low – Low	High	Coincide
184	738717	805963	0.00959	Very low – Low	High	Coincide
185	738724	806266	0.00364	Very low – Low	High	Coincide
186	738017	807073	0.029745	Very low - Low	High	Coincide
187	738049	806961	0.550703	Moderate - High	Low	Coincide

IV. CONCLUSION

In this study, geophysical and hydro-chemical investigations were carried out in the northwestern part of Akure characterized by four rock types: Quartzite, Charnockite, Porphyritic Granite and Granite. The study aims to evaluate the groundwater vulnerability to contamination in the study area using the integration of geologic and geoelectric parameters.

Three to five geoelectric layers namely topsoil, weathered layer, fractured weathered layer, fractured basement and fresh basement were delineated in the study area. The first and second-order information obtained from the geoelectric parameters namely, the overlying layer resistivity of the aquifer unit, the overlying layer thickness of the aquifer unit, hydraulic conductivity and coefficient of anisotropy were combined with surface elevation and lithology in the development of the aquifer vulnerability maps of the study area.

To enhance the accuracy of the aquifer vulnerability model, the fuzzy AHP method was used to determine the weight of the considered parameters where appropriate ratings were assigned to each contributing factor. All data were integrated to form the aquifer vulnerability index (AVI) map for the study area. The calculated aquifer vulnerability index ranges between 1.0494 and 4.4599. The model was able to predict areas with very low vulnerability, low vulnerability, moderate vulnerability, and high vulnerability within the study area using the quantile classification method. In the study, the most effective impact parameter is the lithology whereas the elevation has the lowest significant impact in the vulnerability map.

The northern and southern part of the map comprises of very low to low vulnerability, which is because of the clayey layer overlying the aquifer unit which may have acted as a barrier to further contamination while the eastern and western part of the map consists of high to very high vulnerability. The

physico-chemical analysis results indicate that most of the concentrations levels for all the sampled water are within [77] permissible limits except Lead, Cadmium and chromium which were observed at the upper limits of the standard values, sulphate, manganese, magnesium, and calcium contents were equally observed at the upper limits of [77] standard in the water samples obtained from the area of investigation. The developed aquifer vulnerability map was validated using well and longitudinal conductance data obtained in the study area with 73% and 74% correlation respectively. This indicates that the aquifer vulnerability model map is reliable and precise. This research can serve as a reference for future research in similar geologic terrain and in making hydrogeological and environmental decisions.

ACKNOWLEDGMENT

The authors appreciate students of Applied Geophysics Department, Federal University of Technology, Akure Nigeria who assisted during the data acquisition stage of this work.

References

[1] B. Adesola, K. Ogundipe, K. T. Sangosanya, B. D. Akintola, A. Oluwa, and E. Hassan, "Comparative study on the biosorption of Pb(II), Cd(II) and Zn(II) using Lemon grass (*Cymbopogon citratus*): kinetics, isotherms and thermodynamics". *Chem. Int.,* vol. 2, pp. 89 - 102, 2016.

[2] M. S. Malik, and J. P. Shukla, "Assessment of groundwater vulnerability risk in shallow aquifers of Kandaihimmat Watershed, Hoshangabad, Madhya Pradesh". *J. Geol. Soc. of India*, vol. 93, pp. 199 - 206, 2019.

[3] K. A. Mogaji, H. S. Lim, and K. Abdullar, "Modelling groundwater vulnerability to pollution using optimized DRASTIC model". IOP Conf. Series: *Earth and Env. Sci.*, vol. 20, no. 012002, 2014.

[4] D. N. Obiora, A. E. Ajala, and J. C. Ibuot, "Evaluation of aquifer protective capacity of aquifer unit and soil corrosivity in Makurdi, Benue State Nigeria using electrical resistivity method". *Journal of Earth Sys. Sci.,* vol. 124, no. 1, pp.125 - 135, 2015.

[5] S. Singha, S. Pasupuleti, S. Singha, and V. G. K. Villuri, "An integrated approach for evaluation of groundwater quality 568 in Korba district, Chhattisgarh using geomatic techniques". *J. of Env. Bio*., vol. 38, no. 5, pp. 865 - 872, 2017.

[6] S. Kumar, A. S. Venkatesh, R. Singh, G. Udayabhanu, and D. Saha, "Geochemical signatures and isotopic systematics constraining dynamics of fluoride contamination in groundwater across Jamui District, Indo-Gangetic alluvial plains, India". *Chemosphere*., vol. 205, pp. 493 - 505, 2018, DOI.10.1016/j.chemosphere.2018.04.116

[7] B. E. Oguama, J. C. Ibuot, D. N. Obiora, and M. U. Aka, "Geophysical investigation of groundwater potential, aquifer parameters, and vulnerability: a case study of Enugu State College of Education (Technical)". *Model. Earth Sys. & Env.,* vol. 5, pp. 1123 - 1133, 2019.

[8] O. G. Olaseeni, M. I. Oladapo, G. M. Olayanju, O. J. Dada, and A. R. Oyebamiji, "Groundwater vulnerability assessment using electrical resistivity method in the northern part of Ado-Ekiti, Southwestern Nigeria". In: IOP Conference: *J. of Phy.*, Conference Series. 1299, 2019, DOI.org10.1088/1742-6596/1299/1/12068

[9] O. G. Olaseeni, M. I. Oladapo, and G. M. Olayanju, "Vulnerability assessment of an aquifer in the basement complex terrain of Nigeria using 'LAHBUD' model". *Model. Earth Sys. & Env.*, 2020. doi.org/10.1007/s40808-020-00912-9.

[10] J. W. Weaver, J. E. Hass, and C. B. Sosik, "Characteristics of Gasoline Release in the Water Table Aquifer of Long Island". A Paper Presented at the National Water Association/American Petroleum Institute conference. *Petroleum hydrocarbon Conference and Exposition,* pp. 11, 1999.

[11] World Health Organization. "Guidelines for Drinking Water Quality". WHO Report, Vol. 1 (First addendum to the third edition), 2006.

[12] A. Shahab, Q. Shihua, S. Rad, S. Keita, M. Khan, and S. Adnan, "Groundwater vulnerability assessment using GIS-based DRASTIC method in the irrigated and coastal region of Sindh Province, Pakistan". *Nord. Hydro.*, vol. 50, no. 1, pp. 319 -338, 2019.

[13] I. Babiker, M. A. A. Mohammed, T. Hiyama, and K. Kato, "A GIS-based DRASTIC model for assessing aquifer vulnerability in Kakamigahara Heights, Gifu Prefecture, Central Japan". *Sci. Total Env*., vol. 345, pp. 127 - 140, 2005.

[14] D. Anirban, S. Satiprasad, K. Amlanjyoti, and D. Chakraborty, D. "Index-based groundwater vulnerability mapping using quantitative parameters". *Env. Earth Sci.,* vol. 75, pp. 522, 2016.

[15] D. Machiwal, V. Cloutier, C. Güler, and N. Kazakis. "A review of GIS-integrated statistical techniques for groundwater quality evaluation and protection". *Env. Earth Sci*., vol. 77, pp. 681 - 687, 2018.

[16] S. Sahoo, A. Dhar, A. Kar, and D. Chakraboty. "Index-Based Groundwater Vulnerability Mapping Using Quantitative Parameters". *Env. Earth Sci.,* vol. 75, no. 522, DOI.org/10.1007/s1266 5-016-5395-x, 2016.

[17] K. A. Mogaji. Development of AHPDST vulnerability indexing model for groundwater vulnerability assessment using hydrogeophysical derived parameters and GIS application. *Pure and Applied Geophysics, vol. 2017, no.* 174, pp. 1787 - 1813, 2017, DOI.org/10.1007/s00024-017-1499-9.

[18] G. O. Omosuyi, "Geoelectric assessment of groundwater prospect and vulnerability of

overburden aquifers at Idanre, Southwestern Nigeria". *Ozean J. App. Sci*., vol. 3, no. 1, pp. 19 - 28, 2010.

[19] A. Agyare, G. K. Anornu, and A. T. Kabo-Bah, "Assessing the vulnerability of aquifer systems in the Volta River basin: a case-study on Afram Plains, Ghana". *Model. Earth Sys. Env*., vol. 3, pp. 1141 - 1159, 2017.

[20] J. C. Egbueri, C. N. Mgbenu, and C. N. Chukwu, "Investigating the hydro-geochemical processes and quality of water resources in Ojoto and environs using integrated classical methods". *Model Earth Sys. Env*., vol. 5, pp. 1443 - 1461, 2019.

[21] A. Gredilla, S. F. De Vallejuelo, L. Gomez-Nubla, J. A. Carrero, F. B. De Leao, J. M. Madariaga, and L. F. Silva, "Inorganic analysis and lead isotope ratios for contamination assessment in recreational (Brazilian) parks". *Envi. Sci. Pollut. Res.,* vol. 24, pp. 24333 - 24345, 2017. DOI.org10.1007/s11356-017-9831-6

[22] M. Dutta, J. Saikia, S. R. Taffarel, F. B. Waanders, D. De Medeiros, C. M. Cutruneo, L. F. Silva, and B. K. Saikia, "Environmental assessment and nano-mineralogical characterization of coal, overburden and sediment from Indian coal mining acid drainage". *Geosci. Front., vol.* 8, no. 6, pp. 1285 - 1297, 2018.

[23] E. O. Adigun, and M. O. Olorunfemi. "Integrated geophysical and hydrochemical Investigation of subsoil and groundwater pollution around three cassava processing factories at Ireti-Ayo community, Ilesha, Southwestern Nigeria". *Ife J. of Sci.,* vol. 19, no. 2, 2017.

[24] P. Kumar, K. S. B. Baban, K. D. Sanjit, K. T. Praveen, and C. Ghanshyam, "Index-based groundwater vulnerability mapping models using hydrogeological settings". A critical evaluation Env. Impact Assessment Rev., vol. 51, no. 2015, pp. 38 - 49, 2015.

[25] K. A. Mogaji, and H. S. Lim, "Development of a GIS-based catastrophe theory model (modified DRASTIC model) for groundwater vulnerability assessment". *Earth Sci. Inform,* vol. 10, pp. 339 - 356, 2017.

[26] I. M. Bahkaly, M. M. El-Waheidi, C. Jallouli, and A. T. Batayneh, "Assessment of shallow aquifer salinity in the Aqaba coastal plain using ERT method: A case study of Maqnah region, Northwestern Saudi Arabia". *Env. Earth Sci.*, vol. 74, pp. 2105 - 2114, 2015.

[27] S. O. A. Helmy, F. A. Rehman, H. M. Harbi, T. Cheema, and A. H. Atef, "Using a combined electrical resistivity imaging and induced polarization techniques with the chemical analysis in determining of groundwater pollution at Al Misk Lake, eastern Jeddah, Saudi Arabia". *Arabian J. of Geosci.*, vol. 9, no. 286, 2016, DOI.org/10.1007/s12517-016-2423-9

[28] K. F. Oyedele, and K. U. Ekpoette, "Resistivity attributes of foundation beds in a sedimentary terrain: Implications on geoengineering soil conditions". *American J. of Sci. & Industrial Res.*, vol. 2, no. 5, pp. 734 - 739, 2011.

[29] O. Anomohanran, "Hydrogeophysical investigation of aquifer properties and lithological strata in Abraka, Nigeria". *J. of African Earth Sci.*, vol. 102, pp. 247 - 253, 2015.

[30] T. O. Adeeko, D. O. Samson, and M. Umar, "Geophysical survey of Basement complex terrain using electrical resistivity method for groundwater potential". *World News Nat. Sci*., vol. 23, pp. 154 - 165, 2019.

[31] J. D. Redman, S. M. DeRyck, and A. P. Annan, "Detection of LNAPL pools with GPR, theoretical modeling and surveys of a controlled spill". *Proceedings of the Fifth International Conference on Ground penetrating Radar (GPR'94), Kitchener, Ontario*, pp. 1283 - 1294, 1994.

[32] E. Sener, and S. Sener, "Evaluation of groundwater vulnerability to pollution using fuzzy analytic hierarchy process method". *Environmental and Earth Sciences*, vol. 73, pp. 8405 - 8424, 2015.

[33] A. A. Akinlalu, A. Adegbuyiro, K. A. N. Adiat, B. E. Akeredolu, and W. Y, "Application of Multi-Criteria Decision Analysis in Prediction of Groundwater Resources Potential: A Case of Oke-ana, Ilesa Area, Southwestern, Nigeria". *NRIAG J. of Astro. & Geophy.*, vol. 6, pp. 182 - 200, 2017.

[34] K. A. Mogaji, and S. B. Omobude, "Modeling of geoelectric parameters for assessing groundwater potentiality in a multifaceted geologic terrain, Ipinsa Southwest, Nigeria - A GIS based GODT approach". *NRIAG J. of Astro. & Geophy.,* vol*. 6, no.* 2, pp. 434 - 451, 2017.

[35] A. D. Adebiyi, S. O. Ilugbo, O. E. Bamidele, and T. Egunjobi, "Assessment of aquifer vulnerability using multi-criteria decision analysis around Akure Industrial Estate, Akure, Southwestern Nigeria". *J. of Eng. Res. and Rep.*, vol. 3, no. 3, pp. 1 - 13, 2019.

[36] O. O. Omotola, M. I. Oladapo, and O. J. Akintorinwa, "Modelling assessment of groundwater vulnerability to contamination risk in a typical basement terrain case of vulnerability techniques application comparison study". *Model. Earth Sys. & Env.,* pp. 1 - 28, DOI.org/10.1007/s40808-020-00720-1, 2020.

[37] A. A. Akinlalu, K. A. Mogaji, and T. S. Adebodun, "Assessment of aquifer vulnerability using a developed "GODL" method (modified GOD model) in a schist belt environ, Southwestern Nigeria". *Env. Monitoring Assessment*, pp. 1 - 28, DOI.org/10.1007/s10661-021-08960-z, 2021.

[38] K. A. N. Adiat, M. N. M. Nawawi, and K. Abdullah, "Application of multi-criteria decision analysis to geoelectric and geologic parameters for spatial prediction of groundwater resources potential and

aquifer evaluation". *Pure and App. Geophy.*, vol. 170, pp. 453 - 471, 2013.

[39] O. J. Akintorinwa, M. O. Atitebi, and A. A. Akinlalu. "Hydrogeophysical and aquifer vulnerability zonation of a typical Basement complex terrain: A case study of Odode Idanre Southwestern Nigeria". *Heliyon, vol. 6, no. 8,* e04549, 2020.

[40] G. O. Omosuyi, D. R. Oshodi, S. O. Sanusi, and I. A. Adeyemo, "Groundwater potential evaluation using geoelectrical and analytical hierarchy process modeling techniques in Akure-Owode, Southwestern Nigeria". *Model. Earth Sys. & Env.,* pp. 1 - 14, 2020. DOI.org/10.1007/s40808-020-00915-6.

[41] K. A. Mogaji, O. F. Atenidegbe, I. A. Adeyemo, K. P. Akinmulewo, "Application of GIS-based PROMETHEE data mining technique to geoelectrical derived parameters for aquifer potentiality assessment in a typical hardrock terrain Southwestern Nigeria". *Sust. Water Res. Mgt.*, pp. 1 - 23, 2022. DOI.org/10.1007/s40899-022-00616-1.

[42] I. A. Adeyemo, O. O. Akinro, and A. A. Adegoke, "Geoelectric sounding and hydrochemical analysis for vulnerability assessment of FUTA campus using modified Le Grand model". *Sci. Domain Int., Asian J. of Geol. Res*., vol. 6, no. 3, pp. 172 - 188, 2023.

[43] I. A. Adeyemo, A. A. Adegoke, O. B. Ojo, T. O. Oluwafemi, "Integration of elevation, lithology and geoelectric parameters using analytical hierarchy process for groundwater potential evaluation in part of Akure metropolis, Southwestern Nigeria". *Asian J. of Geol. Res.*, vol. 6, no. 3, pp. 189 - 203, 2023.

[44] A. M. Al-Abadi, and S. A. Shahid, "GIS-based integration of catastrophe theory and analytical hierarchy process for mapping flood susceptibility: a case study of Teeb area. Southern Iraq" *Env. Earth Sci.,* vol. 75, no. 687, 2016.

[45] C. Kahraman, D. Ruan, and I. Dogan, "Fuzzy group decision making for facility location selection". *Info. Sci.*, vol. 157, pp. 135 - 153, 2003.

[46] A. Ozdagoglu, and G. Ozdagoglu, "Comparison of AHP and Fuzzy AHP for the Multi-Criteria Decision-Making Process with Linguistic Elevations". *Istanbul Trade Univ. J. Sci.*, vol. 11, pp. 65 - 85, 2007.

[47] P. J. M. Van Laarhoven, and W. Pedrycz, "A fuzzy extension of Saaty's priority theory". *Fuzzy Set Sys.*, vol. 11, pp. 229 - 241, 1983.

[48] C-N. Lin. "A Fuzzy Analytic Hierarchy Process-Based Analysis of the Dynamic Sustainable Management Index in Leisure Agriculture". *Sustainability, vol. 12*, no. 13.5395, 2020. DOI. 10.3390/su12135395

[49] Y. Mishra, and G. Thakar, "Comparison of Classical Fuzzy Analytic Hierarchy Process and Extended Fuzzy Analytic Hierarchy Process for Vendor Selection in Automobile Supply Chain". *Presented at the National Conference on Emerging Challenges for Sustainable Business*, 2012.

[50] Q. Zhou, J. Su, K. Arnberg-Nielsen, Y. Ren, J. Luo, Z. Ye, and J. Feng. "A GIS-based hydrological modelling approach for rapid urban flood hazard assessment". *Water,* vol. 13, no. 11, pp. 1483, 2021.

[51] O. A. Ogunrayi, F. M. Akinseye, V. Goldberg, and C. Bernhofer, "Descriptive analysis of rainfall and temperature trends over Akure, Nigeria". *J. of Geog. and Reg. Plan.,* vol. 9, no. 11, pp. 195 - 202, 2016.

[52] M. A. Rahaman, "Recent advances in the study of the Basement complex of Nigeria. Precambrian Geology of Nigeria". *A Pub. of Geol. Surv. of Nig.*, pp. 11 - 41, 1988.

[53] M. H. Loke, "Course notes for USGS workshop ''2-D and 3-D inversion and modelling of surface and borehole resistivity data''. Storrs, CT, pp. 13 - 16, 2001.

[54] P. K. Bhattacharya and H. P. Patra, "Direct Current Geoelectric Sounding: Principles and Interpretation". Amsterdam Elsevier, pp. 135, 1968.

[55] V. Vander, "WinRESIST Version 1.0 Resistivity Depth Sounding Interpretation Software". M.Sc. Research Project, ITC, Delft Netherland, 2004.

[56] A. A. Ayman, "Using generic and pesticide DRASTIC GIS-based models for vulnerability assessment of the Quaternary aquifer at Sohag, Egypt". *Egypt Hydrogeol. J.*, vol. 17, pp. 1203 - 1217, 2009.

[57] T. Tomer, D. Katyal, and V. Joshi, "Sensitivity analysis of groundwater vulnerability using DRASTIC method: A case study of National Capital Territory, Delhi, India". *Groundwater Sust. Dev.*, vol. 9, 2019.

[58] P. M. S. Abad, E. Pazira, M. H. M. Abadi, and P. A. Nejad. "Assessment of groundwater vulnerability and sensitivity to Pollution in Aquifers Zanjan Plain". *Iran J. App. Sci. Env. Mgt.*, vol. 21, no. 7, pp. 1346 - 1351, 2017.

[59] H. Baalousha, "Vulnerability Assessment for the Gaza Strip, Palestine Using DRASTIC". *Env. Geol*., vol. 50, pp. 405 - 414, 2006.

[60] M. Samake, Z. Tang, W. Hlaing, M. I. Ndoh, K. Kasereka, and O. B. Waheed, "Groundwater vulnerability assessment in shallow aquifer in Linfen Basin, Shanxi Province, China using DRASTIC model". *Int. J. Sust. Dev., vol.* 4, no. 1, pp. 2011.

[61] K. P. Singh, "A First Attempt for Determination of Relationships between Geophysical Parameters and Yield of the Aquifers". *Presented In 91st Conference of ISC, 3 - 7 January Punjab University,* Chandigarh, India, 2005.

[62] G. M. Olayanju, "Delineation of fault assisted aquifer using tripotential Wenner array-technique around Ita-Oniyan industrial layout, Akure, Nigeria". *Nig. J.* of *Pure & App. Phy., vol.* 2, no. 1, pp. 6 - 16, 2003.

[63] S. O. Olaniyan. Estimation of Aquifer Protective Capacity, Soil Corrosivity and Dar-Zarrouk13

Parameters in Kaura Area of Kaduna State, Nigeria. *Euro. J. of Eng. Res. & Sci.,* vol. 5, no. 10, pp. 1142 - 1151, 2020.
[64] W. Ho, "Integrated Analytic Hierarchy Process and Its Applications - A Literature Review". *Euro. Journ. of Op. Res.*, vol. 186, pp. 211 - 228, 2008.
[65] A. Ishizaka. "Assigning Machines to Incomparable Maintenance Strategies with ELECTRE-SORT". *Omega*, vol. 47, pp. 45 -59, 2014.
[66] Z. L. Yu, L. C. Zhang, and C. W. Zhang, "Web Service Composition Method Based on FAHP and TOPSIS". J. of Comm. & Info. Sci., vol. 2, no. 1, pp. 75 - 84, 2012.
[67] H. C. Huang, "A Novel Site Assessment Model Based on Fuzzy Analytic Hierarchy Process for Water Recreation Activities". Adv. in Info. Sci. & Service Sci., vol. 4, no. 21, pp. 72 - 81, 2012.
[68] Y. P. Du, L. M. Jia, F. Chen, Z. H. Zhang, and Y. Qin, Fuzzy Analytic Hierarchy Process for High-speed Rail Train Plan Evaluation on Special Operation Conditions". J. of Conv. Info. Tech., vol. 6, no. 5, pp. 237 - 244, 2011.
[69] D. Y. Chang, "Applications of the extent analysis method on Fuzzy AHP". *Euro. J. of Op. Res.*, vol. 95, pp. 649 - 655, 1996.
[70] M. L. Tseng, Y. H. Lin, A. S. F. Chiu, and C. Y. Chen, "Fuzzy AHP Approach to TQM Strategy Evaluation". *IEMS, vol.* 7, no. 1, pp.34 - 43, 2008.
[71] C. Kahraman, U. Cebeci, and Z. Ulukan, "Multi-criteria supplier selection using fuzzy AHP". *Log. Infor. Mgt.,* vol. 16, no. 6, pp. 382 - 394, 2003.
[72] D. Dubois, and H. Prade, "Fuzzy Sets and Systems: Theory and Applications". New York: Academic Press, 1980.
[73] A. E. Edet and C. S. Okereke, "Assessment of hydrogeological conditions in basement aquifers of the Precambrian Oban Massif, Southwestern Nigeria". *J. of App. Geophy.*, pp. 195 - 204, 1996.
[74] A. O. Adelusi, M. A. Ayuk, and K. A. N. Adiat, "Evaluation of Groundwater Potential and Aquifer Protective Capacity Assessment at Tutugbua-Olugboyega area, Off Ondo Road, Akure Southwestern Nigeria". *Int. J. of Phy. Sci.*, vol. 8, no. 1, pp. 37 - 50, 2013.
[75] G. F. Jenks, "The Data Model Concept in Statistical Mapping". *Int. Yearbook of Cartography*, vol. 7, pp. 186-190, 1967.
[76] D. Ibrahim, S. U. Abdullahii, I. U. Adamu, L. L. Dazi, A. I. Salihu, and I. A. Simon, "Heavy Metal Contamination of Soil and Ground Water at Automobile Mechanic Workshops in Borno State, Nigeria". *Nig. Res. J. of Chem. Sci., v*ol. 7, 2019.
[77] World Health Organization. "Guidelines for Drinking Water Quality: Fourth Edition Incorporating the First Addendum; WHO: Cham, Switzerland, vol. 631, ISBN 978924154995, 2017.
[78] M. I. Oladapo, and O. J. Akintorinwa, "Hydrogeophysical study of Ogbese Southwestern Nigeria". *Global J. Pure App. Sci.*, vol. 13, no. 1, pp. 55 - 61, 2007.